UNIVERSITÀ DEGLI STUDI DI MILANO

FACOLTÀ DI SCIENZE E TECNOLOGIE

CORSO DI LAUREA MAGISTRALE IN FISICA

HIGHER-ORDER MATCHING FOR HEAVY QUARKS IN PERTURBATIVE QCD

Relatore:
Chiar.mo Prof. Stefano Forte
Correlatore:
Prof. Stefano Carrazza

Tesi di Laurea di:
Silvia Zanoli
Matr. 940018

Anno Accademico 2019/2020

Abstract

A correct treatment of heavy quarks is crucial for a precise description of phenomenology. This thesis analyses the Fixed-Order Next-Leading-Log FONLL approach which defines a general framework for the matching of a calculation in which a heavy quark is treated as a massless parton to one in which the mass dependence is retained throughout. We explicitly consider the case of a deep-inelastic scattering, describing how to include heavy quark mass contributions to deep-inelastic structure functions. We develop the FONLL structure functions up to α_s^3, which means one order higher than the actual FONLL equations, with the basic idea of completely defining - at least theoretically - the FONLL framework at N^3LO, the new frontier for high-precision predictions. The obtained structure functions cannot be numerically studied yet because many Wilson coefficients that are required are analytically known only in the asymptotic region.

We then study in detail the matching condition for the heavy quark, considering the concrete case of the charm. The main purpose is the comparison among the perturbative charm PDF with a α_s^3 matching (our result), a α_s^2 matching and a fitted charm that takes into account also a possible non-perturbative component. Our result is only partial because the coefficients required for the calculation are not fully known; anyway, the most significant part has already been computed, which is sufficient for a first phenomenological study. The charm PDF starts at order α_s^2, which means that we consider the first non trivial correction to the leading order.

Our result shows that the NLO correction to the charm matching condition is particularly high and it has the same shape of the LO contribution: the perturbative series is far from convergence. For investigating the charm content of the proton, one can thus neither fit the charm PDF or consider our result with an error bar that covers the intermediate region between the 2-loop and 3-loop contributions.

Contents

Chapter 1

Introduction

A correct treatment of heavy quarks is essential for precision measurements at hadron colliders. Treating heavy flavours is not trivial because one must take into account the changing role of the heavy quark over the full kinematic range, from the production threshold, where mass effects are important, to the high-energy region, where the heavy flavour can be considered as a massless parton. In order to obtain reliable predictions on the whole kinematic range, these two different frameworks must be matched together and rearranged in a single theory, so that one can define a framework that is accurate at all scales.

In this thesis, we will discuss the Fixed-Order Next-Leading-Log FONLL approach which defines a framework for the inclusion of heavy quark effects in deep-inelastic structure functions. Nowadays, the FONLL approach is commonly used with a perturbative expansion up to α_s^2, where α_s is the strong coupling. In this work we extend the FONLL equations one order higher, with the main goal of completely defining the theoretical framework for a full N^{3}LO matching.

In fact, at hadron colliders such as the LCH, matching the precision of actual data needs a reduction of theory uncertainties, which are dominated by errors related to Quantum Chromodynamics. This reduction requires predictions at or beyond next-to-next-to-leading order (NNLO), which is today's state of heart for fixed order calculations. In particular, the recent N^{3}LO computation [20] of the partonic cross section for the production of a Higgs boson via the fusion of two bottom quarks showed that N^{3}LO is the new frontier for high-precision predictions.

Another key ingredient in QCD is represented by *Parton Distribution*

Functions: a PDF $f_i(x, Q^2)$ represents the probability of finding a parton i carrying a momentum fraction x inside a hadron. A precise knowledge of PDFs is essential in order to make predictions in the Standard Model. In the same vein of reducing the theory uncertainty related to QCD, we will deeply discuss how a α_s^3 matching can modify the charm PDF. At the moment, the matching condition for the charm PDF is known up to α_s^2, which is however just the leading order: the *real* charm PDF can thus be very different.

This thesis is structured as follows: the first chapter is a brief revision of QCD factorization, starting from the important case of electromagnetic deep-inelastic scattering. We also discuss the DGLAP evolution equation. In this same section, we describe an important formalism which will be useful in the next sections: the Operator Product Expansion OPE.

The second chapter is dedicated to the treatment of heavy quarks. We describe how a theory with n_l light quarks and a single heavy flavour can be discussed, using both a *massive* scheme, in which the heavy mass is retained, and a *massless* scheme, in which we consider the heavy flavour as a massless parton. An important section is dedicated to the definition of the perturbative matching conditions between the two schemes.

The third part is dedicated to the FONLL approach: we discuss in detail how to construct the FONLL structure functions and we dedicate a section to the matching condition for the heavy quark, considering the specific case of the charm.

In the last chapter we discuss our results. The first part shows explicitly how to construct the FONLL structure functions up to α_s^3, providing analytic expressions without a numerical implementation. The second part is related to the charm matching condition, which is numerically implemented and compared to the actually known charm PDFs.

Chapter 2

Theoretical background: factorization

Quantum Chromodynamics QCD is the modern theory of strong interactions. It describes the interactions between quarks and gluons, and how they bind together to form hadrons. Precision physics at hadron colliders requires an accurate understanding of QCD over a vast range of scales, which span from the proton mass (~ 1 GeV) to the centre-of-mass energy of the hard scattering processes (few TeV).

The non-abelian nature of QCD, and the consequent asymptotic freedom, permits the calculation of partonic cross sections through perturbation theory in the high-energy limit. By contrast, at lower scales perturbativity breaks down and reliable results can be provided by non-perturbative approaches only. For example, the technique of lattice simulations provided valuable results in this region, thus becoming a well-established basic tool in these calculations.

Even considering the high-energy region only, perturbative QCD could be insufficient for describing data. In general, high-energy cross sections are a combination of high- and low- energy contributions, and thus not directly obtainable through a perturbative approach only. In practice, a direct calculation can be affected by infrared (low-energy) divergences. The predictive power of perturbative QCD is restored thanks to the property of *factorization* of collinear singularities.

Collinear factorization is a general property of QCD which allows one to separate the high-energy, short-distance perturbative contribution to the low-energy, long-distance non-perturbative part in the calculation of a high-

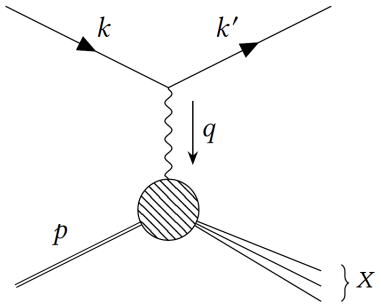

Figure 2.1: Deep-inelastic scattering.

energy cross section. This process can be systematically performed reabsorbing the non-perturbative contributions in universal objects: the parton distribution functions PDFs.

In this chapter we describe how the factorization of collinear singularities works, considering explicitly the case of a deep-inelastic scattering DIS. We then describe an important formalism which will be useful in the next chapters: the operator product expansion.

2.1 Deep Inelastic Scattering

The deep-inelastc scattering is the process in which a lepton scatters off a hadron with the exchange of an electro-weak boson with large virtuality. DIS played, and still plays, an important role in strong-interaction physics, particularly in our understanding of the structure of the nucleon. Furthermore, it provides a rich theoretical and experimental laboratory to quantitatively study and test QCD.

We consider the process depicted in 2.1:

$$l_1(k) + N(p) \to l_2(k') + X \tag{2.1}$$

where a lepton with momentum k scatters off a proton of momentum p. The momentum of the exchanged vector boson is $q = k - k'$. In this analysis we

use the common DIS variables:

$$\begin{aligned} \text{Momentum transfer:} \quad & Q^2 = -q^2 > 0 \\ \text{Energy transfer:} \quad & \nu = p \cdot q \\ \text{Bjorken variable:} \quad & x = \frac{Q^2}{2p \cdot q}, \quad x \in [0,1] \\ \text{Fractional energy transfer:} \quad & y = \frac{q \cdot p}{k \cdot p}, \quad y \in [0,1] \end{aligned} \tag{2.2}$$

At a given centre-of-mass energy s, the differential cross section of the process is expressed as a function of Q^2 and x or x and y. This differential cross section is proportional to the matrix element squared and can be factorized into an hadronic and a leptonic part:

$$\frac{d^2\sigma}{dxdQ^2} \propto L_{\mu\nu} W^{\mu\nu} \tag{2.3}$$

where $L^{\mu\nu}$ is the leptonic tensor and $W^{\mu\nu}$ is the hadronic one.

$$L^{\mu\nu} = \frac{1}{Q^2} \overline{\sum_{spin}} \langle l_1 | j^\mu | l_2 \rangle \langle l_2 | j^{\nu\dagger} | l_1 \rangle \tag{2.4}$$

$$W^{\mu\nu} = \frac{1}{4\pi} \overline{\sum_{spin,X}} \langle P | J^\mu | X \rangle \langle X | J^{\nu\dagger} | P \rangle (2\pi)^4 \delta(P + q - p_X) \tag{2.5}$$

The hadronic tensor contains all the information about the interaction of the conserved current J^μ with the target hadron and, in its definition, the sum is performed over all the final states compatible with the process and the average is done over the incoming elicity states. While the leptonic tensor can be easily calculated, the hadronic one is usually expressed in the most general form introducing the *structure functions* which contains the information about the structure of the hadron as seen by the virtual boson. If we restrict ourselves to the electromagnetic case in which a virtual photon γ^* is exchanged [1], the constraints of Lorentz invariance and current conservation lead to the following parametrization:

$$W^{\mu\nu}(p,q) = \left(-g^{\mu\nu} - \frac{q^\mu q^\nu}{q^2}\right) F_1(x,Q^2) + \left(p^\mu - \frac{p \cdot q}{q^2} q^\mu\right)\left(p^\nu - \frac{p \cdot q}{q^2} q^\nu\right) \frac{1}{p \cdot q} F_2(x,Q^2) \tag{2.6}$$

[1] Considering the exchange of a virtual photon γ^* is correct only if $Q^2 \ll m_W^2$, which means that the transferred energy is not sufficient to produce a massive electro-weak vector boson Z and $W^\pm$.

where F_1 and F_2 are the structure functions. In the general case of an electro-weak interaction, a third structure function F_3 is needed: this new term violates parity.

Defining the *longitudinal structure function* as $F_L = F_2 - 2xF_1$ and explicitly calculating the leptonic tensor, equation (2.3) becomes

$$\frac{d^2\sigma}{dxdQ^2} = \frac{2\pi\alpha^2}{xQ^2}\{[1+(1-y)^2]F_2(x,Q^2) - y^2F_L(x,Q^2)\} \tag{2.7}$$

where α is the fine structure constant.

In early DIS experiments, structure functions were observed to obey an approximate scaling law, the so-called *Bjorken scaling*: in the $Q^2 \to \infty$ region, structure functions depend only on the dimensionless variable x.

$$F_i(x,Q^2) \longrightarrow F_i(x) \tag{2.8}$$

Bjorken scaling implies that the virtual photon scatters off *pointlike constituents*, otherwise the dimensionless structure functions would depend on the ratio Q/Q_0, where $1/Q_0$ is some length scale characterising the size of the constituents. This idea led Bjorken and Feynman to formulate the *parton model*: the basic idea is assuming that a hadron is made up of point-like, non interacting *partons* which carry a fraction x of the momentum of the hadron. For each species a of parton, one can introduce a *parton distribution function* (PDF) $f_a(x)$ which represents the probability that a parton a carries a fraction x of the total momentum of the hadron. In this simple model, structure functions can be obtained considering the scattering of the virtual photon off a single parton, thus obtaining a partonic cross section, and then weighting this term with the parton distribution function. The result must be summed over all the parton species. At leading order in the strong coupling $\mathcal{O}(\alpha_s^0)$, the structure functions become:

$$\begin{aligned} F_2(x) &= \sum_a e_a^2 x f_a(x) \\ F_L(x) &= 0 \end{aligned} \tag{2.9}$$

The second equation is the *Callan-Gross relation*, which is a consequence of the spin-1/2 nature of partons.

Nowadays we interpret the parton model as the leading order of perturbative QCD, in which Bjorken scaling is violated by collinear divergences. In fact, in QCD both virtual and real corrections to a hard process produce

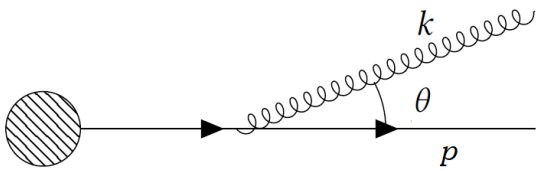

Figure 2.2: Real gluon emission from a quark line.

divergent terms which represent *soft* and *collinear* singularities. In virtual diagrams, divergences appear when integrating the loop momentum on the infrared region while, in real diagrams, singularities appear when integrating over the phase space.

In order to understand the origin of these divergences we can study the splitting of a quark line into a quark and gluon line, as in figure 2.2. If the quark is massless, the internal fermion propagator is proportional to:

$$\frac{1}{(p+k)^2} = \frac{1}{2E_qE_g(1-\cos\theta)} \xrightarrow{\theta\ll 1} \frac{1}{E_qE_g\theta^2} \tag{2.10}$$

which diverges if the energy of the massless gluon goes to zero (soft singularity), or if the angle θ goes to zero (collinear singularity), or both. More precisely, in the soft limit the squared matrix element and the phase space for the gluon emission factorize:

$$|M|^2_{q\bar{q}g}d\phi \sim |M|_{q\bar{q}}d\phi d\omega \tag{2.11}$$

where $d\omega$ is the probability of soft gluon emission in the soft and collinear limit

$$d\omega \sim \frac{dE_g}{E_g}\frac{d\theta^2}{\theta^2} \tag{2.12}$$

Each singularity gives rise to a logarithmic divergence. If we consider a massive quark, we introduce a natural regulator for collinear singularities because the propagator becomes proportional to:

$$\frac{1}{(p+k)^2 - m^2} = \frac{1}{2E_qE_g(1-\sqrt{1-\frac{m^2}{E_q^2}}\cos\theta)} \tag{2.13}$$

For this reason, collinear singularities are also called mass singularities.

Figure 2.3: Real and virtual contribution to the initial state splitting.

These problems related to virtual and real emissions are notably simplified by the KLN theorem [41, 42] which states that fully inclusive observables are free of infrared singularities: for total inclusive observables there is an exact compensation of the real and virtual divergences. In the DIS process, however, the KLN theorem does not hold for the initial state singularities because of the different hard-scattering kinematics (see figure 2.3) of the real and virtual contributions. While soft singularities ($z \to 1$) cancel between real and virtual corrections, collinear divergences remain because the momentum which flows in the hard process is different in the two cases.

To be more precise, the quark momentum which enters the hard scattering is zp in the real contribution while it is p in the virtual correction. This kinematic discrepancy is null only in the soft limit $z \to 1$: the KLN theorem guarantees the disappearance of soft divergences but collinear ones remain.

Specifically considering the DIS scattering, at the lowest order $\mathcal{O}(\alpha_s^0)$ the cross section for the process $\gamma^* q \to q$ is proportional to $e_q^2 \delta(z-1)$. At the first order $\mathcal{O}(\alpha_s)$, both real and virtual QCD corrections arise (see figure 2.4). An

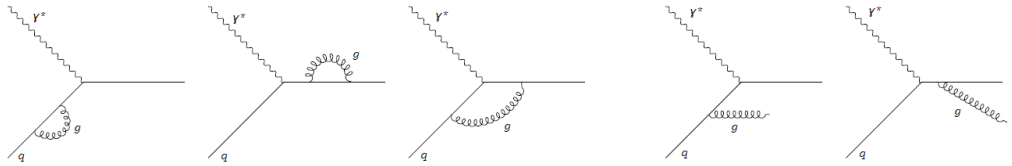

Figure 2.4: Virtual and real contributions at order α_s in the process $\gamma^* q \to q$.

explicit calculation of the partonic cross section at this order shows that the α_s contribution is:

$$\hat{\sigma}^{(1)} = \frac{C_F \alpha_s}{2\pi} \int dz \frac{dk_\perp^2}{k_\perp^2} \frac{1+z^2}{1-z} \left(\hat{\sigma}^{(0)}(zp) - \hat{\sigma}^{(0)}(p) \right) \tag{2.14}$$

where $k_\perp$ is the transverse momentum of the emitted gluon. The soft singularity at z=1 cancels between real and virtual corrections but the collinear singularity $k_\perp \to 0$ does not.

Collinear singularities are treated similarly to UV divergences in a renomarlization procedure: they are reabsorbed into parton distribution functions that, as a consequence, acquire a scale dependence. This process is the *factorization of collinear singularities*.

2.2 Factorization of collinear singularities

The key concept for removing collinear singularities is realizing that the small-$k_\perp$ limit corresponds to a sensitivity to long-range strong interactions which cannot be calculated in perturbative QCD. The parton distribution functions introduced in the parton model are unmeasurable, *bare* quantities and can be redefined in order to reabsorb the divergent terms into *physical* PDFs. Hadronic cross sections can thus be obtained starting from partonic cross sections, which are process-dependent, free of collinear singularities and computable order by order in pQCD, and physical parton densities, which are universal non-perturbative objects that must be extracted from data. The procedure of separation of the high-energy contribution, computable order by order in pQCD, and the low-energy correction, which must be experimentally exctracted, is the factorization.

Turning back to the DIS discussion, equation (2.14) can be rewritten as

$$\hat{\sigma}^{(1)}(x, Q^2) = e_q^2 \alpha_s \left[P(x) \ln \frac{Q^2}{Q_0^2} + C(x) \right] \tag{2.15}$$

where Q_0 is a scale introduced for regularizing the logarithmic divergence, $C(x)$ is a calculable function and $P(x)$ is the so-called splitting function defined as

$$P(x) = C_F \left[\frac{1+x^2}{(1-x)_+} + \frac{3}{2}\delta(1-x) \right]. \tag{2.16}$$

The *plus distribution* is defined so that its integral with any sufficiently smooth distribution f is

$$\int_0^1 dx \frac{f(x)}{(1-x)_+} = \int_0^1 dx \frac{f(x) - f(1)}{1-x} \tag{2.17}$$

and

$$\frac{1}{(1-x)_+} = \frac{1}{1-x} \quad \text{for} \quad 0 \leq \mathrm{x} < 1 \tag{2.18}$$

Considering for simplicity only one parton species, the structure function at the first order in α_s is

$$F(x,Q^2) = e_q^2\left[f^{(0)}(x) + \alpha_s \int_x^1 \frac{dz}{z}\left(P(z)\ln\frac{Q^2}{Q_0^2} + C(z)\right) f^{(0)}(\frac{x}{z}) + O(\alpha_s^2)\right] \tag{2.19}$$

where $f^{(0)}$ represents the bare parton density. The removal of collinear singularities can be performed introducing a *factorization scale* μ_F which allows one to separate the divergent contribution:

$$\ln\frac{Q^2}{Q_0^2} = \ln\frac{Q^2}{\mu_F^2} + \ln\frac{\mu_F^2}{Q_0^2} \tag{2.20}$$

so that equation (2.19) can be rewritten as

$$F(x,Q^2) = e_q^2\left[f^{(0)}(x) + \alpha_s \int_x^1 \frac{dz}{z}\left(P(z)\ln\frac{Q^2}{\mu_F^2} + P(z)\ln\frac{\mu_F^2}{Q_0^2} + C(z)\right) f^{(0)}(\frac{x}{z}) + O(\alpha_s^2)\right] \tag{2.21}$$

The physical PDFs can be obtained introducing a μ_F-dependent term Γ

$$\Gamma\left(z, \frac{\mu_F^2}{Q_0^2}\right) = P(z)\ln\frac{\mu_F^2}{Q_0^2} + \Gamma_{reg}(z) \tag{2.22}$$

so that the μ_F-dependent PDFs are:

$$f(x,\mu_F) = f^{(0)}(x) + \alpha_s \int_x^1 \frac{dz}{z} f^{(0)}\left(\frac{x}{z}\right)\Gamma\left(z, \frac{\mu_F^2}{Q_0^2}\right) + O(\alpha_s^2) \tag{2.23}$$

In equation (2.22), Γ_{reg} represents finite (non-logarithmic) contributions. It is clear that the parton distribution function $f(x,\mu_F)$ cannot be calculated from first principles in perturbation theory, since it receives contributions from the low-energy (non-perturbative) part of the strong interaction. It must be extrapolated from data.

The structure function (2.19) is now straightforward:

$$F(x,Q^2) = e_q^2\left[f(z,\mu_F^2) + \alpha_s \int_x^1 \frac{dz}{z}\left(P(z)\ln\frac{Q^2}{\mu_F^2} + \hat{C}(z)\right) f\left(\frac{x}{z},\mu_F^2\right) + O(\alpha_s^2)\right] \tag{2.24}$$

where $\hat{C}(z)$ depends on the specific choice of the regular part in (2.22).

It is important to underline that while factorization provides a prescription for dealing with the logarithmic singularities, there is an arbitrariness on the treatment of regular terms. How much finite contributions are factored out defines the *factorization scheme*. A common choice for the factorization scheme is the Modified Minimal Subtraction $\overline{MS}$ scheme, in which in addition to the divergent piece, a $(\ln 4\pi - \gamma_E)$ contribution is absorbed into the parton distribution.

In general, the finite contributions that remain after the factorization process are collected by defining a *coefficient function* $C(z, \frac{Q^2}{\mu_F^2})$; the structure function can thus be expressed as:

$$F(x,Q^2) = e_q^2\left[f(z,\mu_F) + \alpha_s \int_x^1 \frac{dz}{z} f\left(\frac{x}{z},\mu_F\right) C^{(1)}\left(z,\frac{Q^2}{\mu_F^2}\right)\right] \tag{2.25}$$

where the superscript $^{(1)}$ refers to the first perturbative order in the strong coupling. In fact, coefficient functions can be computed order by order in perturbation theory as an expansion in α_s:

$$C(x,\alpha_s) = C^{(0)}(x) + \alpha_s C^{(1)}(x) + \alpha_s^2 C^2(x) + ... \tag{2.26}$$

So far, we considered the specific case of a DIS process at the first order in α_s with a single partonic species. This discussion can be extended considering that, in a general case, structure functions are obtained considering all the partonic species which enters the process at a desired order: equation (2.25) must then contain all the information carried by the different active flavours and the gluon.

$$F(x,Q^2) = \sum_a \int_x^1 \frac{dz}{z} C_a\left(\frac{x}{z},\frac{Q^2}{\mu_F^2},\alpha_s\right) f_a(z,\mu_F^2) \tag{2.27}$$

In a compact form, equation (2.27) can be express introducing the convolution symbol $\otimes$:

$$F(x,Q^2) = \sum_a C_a\left(x,\frac{Q^2}{\mu_F^2},\alpha_s\right) \otimes f_a(x,\mu_F^2) \tag{2.28}$$

Structure functions are thus obtained as the convolution between coefficient functions, which are computable order by order in perturbation theory and represent the high-energy contributions to the process, and parton distribution functions, which are universal non-perturbative objects that must be extrapolated from data. Furthermore, equation (2.28) explicitly shows that Bjorken scaling is broken in QCD by logarithms of the hard scale Q.

In this section we showed how factorization is a key concept in QCD that enables one to apply perturbative calculations in many important processes involving hadrons: the factorization procedure consists in a systematic separation between low- and high- energy contributions in the calculation of hard processes through the definition of physical parton distribution functions which reabsorb divergent terms. Several arguments show that factorization can be performed at all orders in perturbation theory, even if a solid proof is present only for specific cases (for example, a DIS scattering). Anyway, the factorization theorem is now widely accepted.

The factorization procedure necessarily requires the introduction of a new scale in the theory. The first-principles calculation of the parton distributions is beyond the scope of perturbation theory, however what can be calculated is how they depend on the factorization scale μ_F. This scale dependence is described by the DGLAP evolution equation.

2.3 DGLAP evolution equation

In the previous section we saw how the factorization procedure requires the introduction of a new scale in the theory: the factorization scale μ_F. The physical parton distribution functions PDFs depend on this scale through the DGLAP equation. To see how to obtain this evolution equation, one can notice that the right-hand side of equation (2.24) does not depend on the factorization scale because structure functions must be independent of μ_F^2:

$$\mu_F^2 \frac{\partial}{\partial \mu_F^2} F(x, Q^2) = 0 \tag{2.29}$$

This constraint leads to a renormalization group equation for the parton density $f(x, \mu_F^2)$:

$$\mu_F^2 \frac{\partial}{\partial \mu_F^2} f(x, \mu_F^2) = \alpha_s(\mu_F^2) \int_x^1 \frac{dz}{z} P\left(\frac{x}{z}\right) f(z, {\mu_F}^2) \tag{2.30}$$

This equation is known as the Dokshitzer-Gribov-Lipatov-Altarelli-Parisi equation [43]. The splitting function P can be calculated order in perturbation theory as an expansion in the running coupling:

$$P(z,\alpha_s) = P^{(0)}(z) + \alpha_s P^{(1)}(z) + \alpha_s^2 P^{(2)}(z) + O(\alpha_s^3) \tag{2.31}$$

Strictly speaking, equation (2.30) is correct only in the case of a theory in which quarks of a single flavour radiate gluons. However, in a complete theory one must take into account the presence of gluons and antiquarks in the target hadron and the different active flavours of quarks/antiquarks. The DGLAP equation is in fact a $(2n_f{+}1)$-dimensional matrix equation in the space of quarks, antiquarks and gluons:

$$\begin{aligned}\mu^2\frac{\partial}{\partial\mu^2}\begin{pmatrix} q_i(x,\mu^2) \\ g(x,\mu^2)\end{pmatrix} = \alpha_s(\mu^2)\sum_{q_j,\bar{q}_j}\int_x^1\frac{dz}{z} \\ \times\begin{bmatrix} P_{q_iq_j}\left(\frac{x}{z},\alpha_s(\mu^2)\right) & P_{q_ig}\left(\frac{x}{z},\alpha_s(\mu^2)\right) \\ P_{gq_j}\left(\frac{x}{z},\alpha_s(\mu^2)\right) & P_{gg}\left(\frac{x}{z},\alpha_s(\mu^2)\right)\end{bmatrix}\begin{pmatrix} q_j(z,\mu^2) \\ g(z,\mu^2)\end{pmatrix}\end{aligned} \tag{2.32}$$

where we dropped the subscript F to the factorization scale. Each splitting function is again calculable as a power series in α_s:

$$\begin{aligned} P_{q_iq_j}(z,\alpha_s) &= \delta_{ij}P_{qq}^{(0)}(z) + \alpha_s P_{q_iq_j}^{(1)}(z) + ... \\ P_{qg}(z,\alpha_s) &= P_{qg}^{(0)}(z) + \alpha_s P_{qg}^{(1)}(z) + ... \\ P_{gq}(z,\alpha_s) &= P_{gq}^{(0)}(z) + \alpha_s P_{gq}^{(1)}(z) + ... \\ P_{gg}(z,\alpha_s) &= P_{gg}^{(0)}(z) + \alpha_s P_{gg}^{(1)}(z) + ... \end{aligned} \tag{2.33}$$

Thanks to charge conjugation invariance and SU(n_f) flavour symmetry, the following identities are valid:

$$\begin{aligned} P_{q_iq_j} &= P_{\bar{q}_i\bar{q}_j} \\ P_{q_i\bar{q}_j} &= P_{\bar{q}_iq_j} \\ P_{q_ig} &= P_{\bar{q}_ig} \equiv P_{qg} \\ P_{gq_i} &= P_{g\bar{q}_i} \equiv P_{gq} \end{aligned} \tag{2.34}$$

i.e. the splitting functions P_{qg} and P_{gq} are independent of the quark flavour and the same for quarks and antiquarks. The leading order $P_{q_iq_j}$ splitting

function is zero unless $q_i = q_j$. This allows the matrix equation (2.32) to be considerably simplified at this order.

The DGLAP equation describes the evolution of the PDFs with the factorization scale μ_F. Given a boundary condition, DGLAP evolution allows one to obtain the behaviour of the PDFs at a generic scale μ. In practice, knowing the PDFs at some initial scale μ_0, equation (2.32) predicts how the PDFs change from the scale μ_0 to any other scale μ.

2.4 Operator Product Expansion

In this section, we describe an important formalism which will be useful in the following chapters: the *Operator Product Expansion* (OPE), also called *Wilson expansion*.

The operator product expansion is a technique used for the calculation of the product of local operators when their separation $|x|$ goes to zero. In quantum field theory, for many applications one needs to compute products of some operators. As we will see, an important example is the calculation of the hadronic tensor in DIS, which can be reduced to the computation of the product of two electromagnetic currents.

If we consider two local operators O_1 and O_2, the Wilson expansion expresses the product of these two operators as a linear combination of local operators of the theory weighted for some coefficients:

$$O_1(x)O_2(0) \to \sum_n C_{12,n}(x)O_n(0) \tag{2.35}$$

The coefficients $C_{12,n}$ are c-number functions while O_n represents a full set of operators of the theory. The interesting aspect is that all the x-dependence is embedded in the coefficients $C_{12,n}$.

Using the OPE, a generic product between operators can be factorized into universal $|x|$-dependent c-number functions and operators. Applying the OPE consists thus in evaluating the universal coefficients and studying all the operators of a theory. As for the coefficients, one must notice that (2.35) is valid on generic states of the Fock space and that the coefficients C_n do not depend on the specific states. In order to calculate these coefficients, one can thus perform a calculation of the form

$$\langle\psi|O_1(x)O_2(0)|\psi\rangle \tag{2.36}$$

where $|\psi\rangle$ is a *simple* state, i.e. a state over which we can make analytic calculations, and then use the universal coefficients for calculating the operator product on the states of interest.

We can now analyse the full set of operators of the theory. Operators can be classified using dimensional analysis: both the right and left members of equation (2.35) must have the same dimensions. For example, if we consider the product of two equal operators, each of which with dimension d_j in terms of length, all the members on the right hand side must have the same dimension:

$$[C_n O_n] \sim [x]^{2d_j} \tag{2.37}$$

If we consider $[O_n] \sim [x]^{d_n}$, we obtain the dimension of the coefficient C_n:

$$[C_n] \sim [x]^{2d_j - d_n} \tag{2.38}$$

In the limit in which the separation goes to zero, operators with a big and negative dimension in terms of length are suppressed, because the related coefficients are suppressed.

In general, operators can have an arbitrary small dimension in terms of length, or equivalently an arbitrary large dimension in terms of mass. Equation (2.38) thus states that the number of operators which contributes in the calculation is rather small.

An important feature must now be underlined: we are working in a Minkowski space, not in an Euclidean one. This fact represents a complication: considering that the norm of a vector $|x|$ tends to zero is not equivalent to the requirement that each of the components of the 4-vector goes to zero independently. More precisely, $x_\mu x^\mu$ can tend to zero with finite x_0 and x_i. If we want to apply the dimensional analysis described before, we must distinguish between two cases: operators which depend on $|x|$ and operators which depend on x^μ.

Let's consider as a simple example the product of two scalar currents:

$$J(x)J(0) = \sum_n C_n O_n \tag{2.39}$$

Coefficients can be scalars, vectors and tensors:

$$\begin{aligned} C_n(x) &= f_n(|x|) \\ C_n^\mu(x) &= x^\mu g_n(|x|) \\ C_n^{\mu\nu}(x) &= x^\mu x^\nu h_n(|x|) \end{aligned} \tag{2.40}$$

in which f_n have the same dimensions of C_n, g_n have the same dimension of C_n^μ minus one, h_n the same as $C_n^{\mu\nu}$ minus two, and so on. We are considering the case in which $|x|$ tends to zero, but x^μ is finite: with coefficients with the same dimensions, g_n goes to zero slower than f_n, and h_n even slower than g_n. The correct dimension in Minkowski space is thus:

$$C_n \sim |x|^{2d_j + d_n - s} \tag{2.41}$$

where s represents the number of indexes of the operator under consideration (it is its spin). The dimension of an operator in terms of mass minus its spin defines the twist t:

$$|d_n| - s = t \tag{2.42}$$

If in the euclidean case the dominant contribution in the calculation comes from operators with the lowest dimension, in the minkovskian case the dominant contribution comes from operators with the lowest twist.

In a theory with fermion fields of dimension 3/2 and gauge fields with dimension 1, operators with lowest twist have dimension 2. In particular, we can consider two different types of operator: in the fist case, they are obtained starting from bilinear fermion fields:

$$\bar{\psi}\gamma^\mu\psi \qquad \mathrm{d} = 3, \mathrm{s} = 1, \mathrm{t} = 2 \tag{2.43}$$

and we have also operators obtained from gauge fields of the form

$$F^{\mu\alpha}F^\nu_\alpha \qquad \mathrm{d} = 4, \mathrm{s} = 2, \mathrm{t} = 2 \tag{2.44}$$

In QCD the number of operators of the form (2.43) is related to the number of colours and flavours in the theory.

Operators with the lowest twist are called *leading twist operators*.

We can now see how this formalism works explicitly considering the calculation of the hadronic tensor $W^{\mu\nu}$ in equation (2.5):

$$W^{\mu\nu} = \overline{\sum}\langle P|J^\mu|X\rangle\langle X|J^{\nu\dagger}|P\rangle(2\pi)^4\delta(P + q - p_X) \tag{2.45}$$

where for simplicity we removed the $1/4\pi$ factor. We introduce an integral representation of a 4-dimensional delta, obtaining:

$$W^{\mu\nu} = \overline{\sum}\int d^4x e^{iq\cdot x}\langle P|J^\mu|X\rangle\langle X|J^{\nu\dagger}|P\rangle \tag{2.46}$$

We can eliminate the dependence on the final state $|X\rangle$ using the optical theorem [26], through which one can express the relation between forward scattering amplitudes and total cross sections. Considering the matrix element from an initial state $|P\gamma^*\rangle$ (proton and virtual photon) and a generic final hadronic state $|X\rangle$

$$iT = \langle X|P\gamma^*\rangle = \langle X|J^\nu|P\rangle\epsilon_\nu \tag{2.47}$$

and applying the optical theorem (J^ν is the electromagnetic current that creates the photon), one can express the hadronic tensor as:

$$W^{\mu\nu} = \frac{2}{\pi}\mathfrak{Im}\int d^4x e^{iq\cdot x}\langle P\gamma^*|P\gamma^*\rangle = \frac{2}{\pi}\mathfrak{Im}\int d^4x e^{iq\cdot x}\langle P|T(J^\mu(x)J^\nu(0))|P\rangle \tag{2.48}$$

thus removing the dependence on the final hadronic state. T is the chronological product. The π at the denominator comes from the correct covariant normalization of physical states.

The difficulties in performing this calculation are related to the evaluation of the product of the currents on a proton state $|P\rangle$. This problems are solved using the operator product expansion.

We now want to study how to calculate $T^{\mu\nu}$ defined as:

$$T^{\mu\nu} = \langle P|T(J^\mu(x)J^\nu(0)|P\rangle \tag{2.49}$$

Of course, the decomposition of the hadronic tensor in (2.6) holds also for $T^{\mu\nu}$, so that one can introduce functions T_i which play the same role of the structure functions in the hadronic tensor:

$$T^{\mu\nu}(p,q) = \left(-g^{\mu\nu} - \frac{q^\mu q^\nu}{q^2}\right)T_1(x,Q^2) + \left(p^\mu - \frac{p\cdot q}{q^2}q^\mu\right)\left(p^\nu - \frac{p\cdot q}{q^2}q^\nu\right)\frac{1}{p\cdot q}T_2(x,Q^2)$$
$$F_i = \frac{2}{\pi}\mathfrak{Im}T_i \tag{2.50}$$

Using the OPE formalism we should consider a complete twist-2 basis of operators in the theory: in order to simplify the calculation, we will consider only fermionic operators. The chronological sorting can be removed thanks to the OPE (the product is seen as the sum of single operators). We can write the expansion of the product:

$$J^\mu(x)J^\nu(0)\sum_{k=2,k=even}^{\infty} O^{\mu\nu\mu_1\dots\mu_{k-2}}x_{\mu_1}\dots x_{\mu_{k-2}}C^k(|x|) \tag{2.51}$$

where the sum is performed only on even k for parity invariance. We have now to consider this expression on a proton state $|P\rangle$.

Firstly, one can observe that the matrix element $\langle P|O^{\mu\nu\mu_1\cdots\mu_{k-2}}|P\rangle$ does not depend on the separation x. All the x dependence is included in the coefficients C^k. In Fourier space, x becomes q, the transferred momentum. The result depend both on q and p, where p is the proton momentum. This means that the operator matrix element can depend only on the proton momentum p, which thus carries the vectorial indexes:

$$\int d^4x e^{iqx}\langle P|T(J^\mu J^\nu|P\rangle = \sum_{k=2}^{\infty} 2p^\mu p^\nu p^{\mu_1}...p^{\mu_{k-2}} A_k \int d^4x e^{iqx} x_{\mu_1}...x_{\mu_{k-2}} C^k(|x|) \tag{2.52}$$

The factor 2 is a normalization and A_k defines the reduced matrix element, the scalar contribution of the operator. We can calculate the Fourier transform introducing the conjugate vectors that must be divided for Q^2 for dimensional analysis:

$$\int d^4x e^{iqx}\langle P|T(J^\mu J^\nu|P\rangle = \sum_{k=2}^{\infty} 2p^\mu p^\nu p^{\mu_1}...p^{\mu_{k-2}} A_k \frac{2q_{\mu_1}}{Q^2}...\frac{2q_{\mu_{k-2}}}{Q^2} C_k(Q^2)\frac{1}{Q^2} \tag{2.53}$$

The previous equation can be rewritten as follows[2]:

$$\int d^4x e^{iqx}\langle P|T(J^\mu J^\nu|P\rangle = \sum_{k=2}^{\infty} A_k C_k(Q^2)\frac{2p^\mu p^\nu}{Q^2}\left(\frac{2p\cdot q}{Q^2}\right)^{k-2} \tag{2.54}$$

where we recognize the Bjorken variable $x = Q^2/2pq$.

Comparing this equation with the explicit expression of $T^{\mu\nu}$ in terms of coefficient functions T_i (2.50), one can conclude that

$$T_2 = \sum_{k=2} A_k C_k(Q^2)\left(\frac{2p\cdot q}{Q^2}\right)^{k-1} \tag{2.55}$$

T_2 is thus a Laurent series in $\omega = 1/x$ and we can thus extract the k-th coefficient of the expansion using Cauchy's formula:

$$A_k C_k = \frac{1}{2\pi i}\oint d\omega \omega^{-k} T_2(x, Q^2) \tag{2.56}$$

[2]Expression (2.54) is easier than the correct one, because a term proportional to $g^{\mu\nu}$ arises due to orthogonality. This term is completely defined by gauge invariance.

T_2 presents two branch cuts (see discussion in chapter 18.5 in [49]) but taking the imaginary part, as required by (2.50), we obtain a finite result. In particular, one finds:

$$A_k C_k = \int_0^1 dx x^{k-1} \left(\frac{F_2(x)}{x} \right) \tag{2.57}$$

This equation is a fundamental result of perturbative QCD: if we take the k-th momentum of the structure function F_2, we obtain a Wilson coefficient $C_k(Q^2)$, explicitly computable in perturbation theory, and the matrix element of an operator $O^{\mu\nu\mu_1 \cdots \mu_{k-2}}$ on proton states. For example, if we consider $k = 2$, we have

$$\int F_2(x) = C_2(Q^2) A_2 \tag{2.58}$$

where A_2 is related to $O_2^{\mu\nu} = \bar{\psi} \gamma^\mu \partial^\nu \psi$.

In this way, we reobtained the crucial property of factorization in perturbation theory using the operator product expansion formalism: if one considers the following Mellin transforms for the Wilson coefficient and the reduced operator matrix element

$$C_k(Q^2) = \int_0^1 dx C(x, Q^2) x^{k-1} \qquad A_k = \int_0^1 f(x) x^{k-1} \tag{2.59}$$

the structure function can be rewritten exactly as defined in (2.27):

$$F_2(x, Q^2) = x \int_x^1 \frac{dz}{z} C\left(\frac{x}{z}, Q^2 \right) f(z). \tag{2.60}$$

This analysis is simpler than the real QCD discussion, in which one must take into account the contributions of both quark and gluon operators, the different flavours and colours. Anyway, the power of this result is clear: we wrote the structure functions as a the product of a Wilson coefficients, which are computable in perturbation theory, and non-perturbative terms embedded in the reduced matrix elements.

Chapter 3

Treatment of heavy quarks

In the previous chapter we provided a detailed description of the factorization procedure. So far, we have worked under the hypothesis of massless quarks but this assumption is unsatisfactory when the hard scale of the process Q is comparable to the quark mass: in this case, the use of a mass-independent scheme such as a $\overline{MS}$ scheme is not justified and precision predictions require the inclusion of heavy quark mass corrections when $Q \sim m_h$.

In general, the up, down and strange quarks can always be considered as massless partons, while for the charm, bottom and top quarks we must allow for the effects of their mass m_h. More precisely, we can distinguish *heavy* and *light* quarks using the typical scale of strong interactions, namely 1 GeV: particles with a higher mass are heavy quarks while the others are light ones.

The basic problem in treating heavy quarks is that a precise analysis must properly take into account the changing role of the heavy quark over the full kinematic range of the relevant process, from the threshold region - where the quark behaves like a heavy particle - to the asymptotic region - where the same quark behaves effectively like a parton similar to light quarks. Precise results for a process at a certain perturbative scale Q^2 require thus matching these two different behaviours, which means including heavy quark mass effects near the threshold region $Q^2 \sim m_h^2$ and the resummation of large collinear logarithms for $Q^2 \gg m_h^2$.

Nowadays, different techniques incorporate both approaches in a unified framework in perturbative QCD which provides a smooth transition between the two schemes. In particular, in this thesis we focus on how to include heavy quark mass contributions to deep-inelastic structure functions.

In this section we will discuss the two main schemes used in the compu-

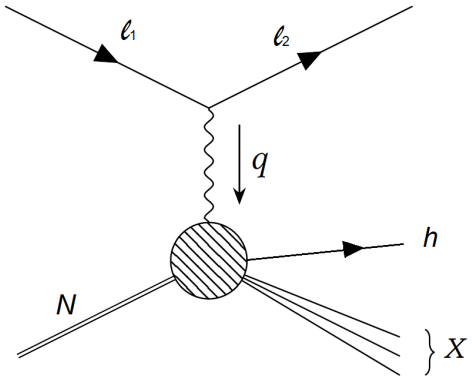

Figure 3.1: Deep inelastic scattering process with the production of a heavy quark h.

tation of deep-inelastic structure functions in the presence of a heavy quark, the so-called *fixed flavour number scheme* (FFNS) and the *variable flavour number scheme* (VFNS).

3.1 FFNS and VFNS

In order to understand how the inclusion of heavy quark mass effects works in deep inelastic scattering, we consider a general DIS process in which we explicitly require the presence of a heavy quark h in the final state.

$$l_1(k) + N(p) \to l_2(k') + h(p_h) + X(p_X) \tag{3.1}$$

In the final state there is an heavy quark h of momentum p_h^μ and mass m_h which has been explicitly separated from the final total hadronic state X':

$$X'(P') = h(p_h) + X(P_X).$$

The process is mediated by a virtual photon γ^* of momentum q.

From now on, we will consider only *heavy* structure functions (*i.e.* with a heavy quark in the final state) up to the first order in α_s, in order to avoid unnecessary complications due to higher-order corrections. At this order,

using the factorization theorem the DIS heavy structure functions reduce to:

$$\begin{aligned} F_k(x,Q^2) &= \sum_{i=g,h,\bar{h}} \int_x^1 \frac{dz}{z} C_{k,i}(\frac{x}{z}, Q^2, \alpha_s(\mu^2)) f_i(z,\mu^2) = \\ &= \sum_{i=h,\bar{h}} C_{k,i}^{(0)} \otimes f_i + \alpha_s \sum_{i=g,h,\bar{h}} C_{k,i}^{(1)} \otimes f_i \end{aligned} \tag{3.2}$$

where the coefficient functions $C_{k,i}$ have been perturbatively expanded in terms of the running coupling α_s. The sum runs over the heavy quark and the gluon PDFs because only gluon-initiated and heavy quark-initiated diagrams contribute to the heavy structure functions up to α_s. The gluon contribution to the coefficient function at LO is zero, since no gluon-initiated graphs contribute at α_s^0.

Coefficient functions in equation (3.2) can be computed in perturbation theory using two different approaches, each of which has a better accuracy in a certain kinematic region. At high scales, i.e. $Q^2 \gg m_h^2$, the heavy quark is expected to behave like a massless parton. Therefore, it is possible to calculate the coefficient functions $C_{k,i}$ explicitly setting to zero the masses of the internal lines and the external partons in graphs for partonic subprocesses. The calculation now presents collinear divergences which can be subtracted in a $\overline{MS}$ scheme. These singularities arising from setting $m_h = 0$ reflect the presence of large collinear logarithms $log(\frac{Q^2}{m_h^2})$: the natural way to resum these contributions is to reabsorb them into the heavy quark PDF f_h which, as a consequence, start evolving according to the DGLAP equation. Using this strategy, one obtains structure functions in the so-called *zero-mass* (ZM) scheme:

$$\begin{aligned} F_k^{ZM}(x,Q^2) &= \sum_{i=g,h,\bar{h}} \int_x^1 \frac{dz}{z} C_{k,i}^{ZM}(\frac{x}{z}, Q^2, \alpha_s(\mu^2)) f_i(z,\mu^2) = \\ &= \sum_{i=h,\bar{h}} C_{k,i}^{ZM,(0)} \otimes f_i + \alpha_s \sum_{i=g,h,\bar{h}} C_{k,i}^{ZM,(1)} \otimes f_i \end{aligned} \tag{3.3}$$

where $C_{k,i}^{ZM}$ are the zero-mass $\overline{MS}$ coefficient functions.

Coefficient functions and DGLAP evolution equation depend on the number of active flavours n_f alike: this yields the so-called Zero-Mass Variable Flavour Number scheme ZMVFNS. The notion *variable flavour number* is used since the number of active quark flavours is increased by one unit,

$n_l \to (n_l + 1)$, when the energy scale crosses certain transition scales, which are usually taken equal to the heavy quark mass. The ZMVFNS works well if the scale Q is much greater than the heavy quark threshold. If we consider a scale $Q^2 \simeq m_h^2$, this scheme is not accurate because it neglects potentially important terms proportional to m_h^2/Q^2.

Alternatively, one can perform calculations retaining the full dependence of the quark mass m_h in the coefficient functions $C_{k,i}$. In this case, resummation of large logarithms is not required because the heavy quark mass m_h is a regulator for the IR divergences. Considering the heavy quark as the $(n_l + 1)$-th flavour, calculations at a scale $Q^2 < m_h^2$ can be performed in the ZM n_l flavour scheme: in this way, the heavy quark decouples from the evolution of the running coupling and the DGLAP evolution of the PDFs, which are equal to the $\overline{MS}$ scheme with n_l flavours. The structure functions become

$$\begin{aligned} F_k^{FF}(x, Q^2) &= \int_x^1 \frac{dz}{z} C_{k,g}^{FF}(\frac{x}{z}, Q^2, \alpha_s(\mu^2), m_h) f_g(z, \mu^2) = \\ &= \alpha_s C_{k,g}^{FF,(1)} \otimes f_g \end{aligned} \tag{3.4}$$

where it is clear that the heavy quark PDFs is no longer present in the calculation. This procedure defines the so called Fixed Flavour Number Scheme FFNS: it basically consists in fixing the number of active flavours n_l and keeping the mass contribution of the $(n_l + 1)$-th flavour in the coefficient functions for scales above the heavy quark threshold. This scheme is not accurate in the region $Q^2 \gg m_h^2$ because of unresummed collinear logarithms.

The ZMVFNS and the FFNS are two distinct schemes which are individually unsatisfactory over the full energy range, but are mutually complementary. From now on, we will simply refer to these schemes respectively as *massless* (or *$(n_l + 1)$-flavour scheme*) and *massive* (or *n_l-flavour scheme*) scheme. Reliable predictions in perturbative QCD can be obtained using a composite procedure that can smoothly interpolate between these two approaches, so that one can use a single accurate scheme over a wide range of energy scales. Techniques which are able to combine the massless and the massive scheme are commonly defined as General Mass Variable Flavour Number Scheme.

It must be underlined that the massive and the massless schemes are not independent: they can be related perturbatively considering how the running coupling and the PDFs are connected in the two schemes. For instance, a

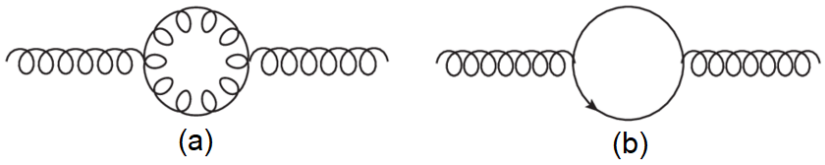

Figure 3.2: Graphs which contribute to the β-function in the one-loop approximation.

generic observable can be expressed in both frameworks as a perturbative expansion in the coupling (in the correct scheme): if the relation between the n_l and $(n_l + 1)$ coupling is known, the coefficients of the perturbative expansion can be matched order by order.

3.2 Matching conditions

The calculation of the perturbative matching conditions that relate the n_l and $(n_l + 1)$ schemes at a specific matching scale μ_{match} is a key ingredient in the definition of a GMVFNS. These matching conditions express the relations between the running coupling and the PDFs in the two frameworks.

The matching relation for the coupling is obtained studying the evolution of α_s through the renormalization group equation in the two schemes, which is determined by the β-function of the theory.

$$\mu^2 \frac{\partial \alpha_s}{\partial \mu^2} = \beta(\alpha_s) \tag{3.5}$$

The β-function admits a perturbative expansion of the form

$$\beta(\alpha_s) = -\beta_0 \alpha_s^2 + \beta_1 \alpha_s^3 + \beta_2 \alpha_s^4 + ... \tag{3.6}$$

where the coefficients β_i can be calculated in perturbation theory.

β is extracted from the higher-order corrections to the bare vertices of the theory and thus it assumes a different value when switching form the n_l scheme to the $(n_l + 1)$ one. A clear example is depicted in 3.2: these graphs contribute to the β-function in the one-loop approximation. When changing scheme $n_l \to (n_l + 1)$, the number of active flavours that circulate in the fermion loop (figure (b)) changes, which determines a difference in the calculation of the β-function in the two theory: β explicitly depends on the

number of active flavours. The β-function is currently known up to five-loop corrections [44].

Comparing order by order in perturbation theory the evolution of the coupling in the massless and in the massive schemes, one can find the matching relation:

$$\alpha_s^{(n_l+1)}(\mu^2_{match}) = \alpha_s^{(n_l)}(\mu^2_{match}) + \Delta\alpha_s \tag{3.7}$$

in which $\Delta\alpha_s$ is a calculable function with a perturbative expansion of the form:

$$\Delta\alpha_s = \sum_{i=2}^{\infty} c_i(L)(\alpha_s^{n_l}(\mu^2_{match}))^i \tag{3.8}$$

where $c_i(L)$ are polynomials which depends on $\log(\mu^2_{match}/m_h^2)$. For example, considering only the first perturbative correction, c_1 can be written as

$$c_1(L) = A\log(\mu^2_{match}/m_h^2), \tag{3.9}$$

where A is a function independent on the matching scale.

The matching scale is usually taken equal to the mass of the heavy flavour m_h for a question of naturalness: this choice is somehow arbitrary but it simplifies substantially the calculation because all the terms proportional to powers of $\log(\mu^2_{match}/m_h^2)$ vanish. In fact, thanks to equation (3.9), at leading order the running coupling is continuous when switching from the n_l to the (n_l+1) description:

$$\alpha_s^{(n_l+1)}(\mu^2_{match}) = \alpha_s^{(n_l)}(\mu^2_{match}) + O({\alpha_s^{(n_l)}}^2). \tag{3.10}$$

Expression (3.7) can be used to relate the coefficients of the perturbative expansion of a generic observable $F(\alpha_s)$ in the two schemes

$$F(\alpha_s) = \sum_k \left(\alpha_s^{(n_l)}\right)^k {F^{(n_l)}}^k = \sum_k \left(\alpha_s^{(n_l+1)}\right)^k {F^{(n_l+1)}}^k \tag{3.11}$$

by expanding and matching the two expressions order by order once both are written in terms of the coupling in the same scheme. In fact, one can consider that a generic structure function $F(x,Q^2)$ can be expressed both in the massless and in the massive scheme, respectively $F(x,Q^2)^{(n_l+1)}$ and $F(x,Q^2)^{(n_l)}$. These two structure functions are not independent, because they represent the same physical quantity. More precisely, they must be equal

order by order in the high energy limit up to power-suppressed contributions. In the n_l scheme, the structure function reads:

$$F^{(n_l)}(Q^2, m_h^2) = \sum_{i=q,\bar{q},g} C_i^{(n_l)}\left(\frac{m_h^2}{Q^2}, \alpha_s^{(n_l)}(Q^2)\right) \otimes f_i^{(n_l)}(Q^2) \tag{3.12}$$

For simplicity, we considered the hard scale equal to the factorization scale $Q^2 = \mu^2$. The coefficient functions $C_i^{(n_l)}$ are calculated factorizing only collinear divergences associated to massless quarks, while radiative corrections which involve the massive flavour are infra-red finite. The PDFs evolve according to the DGLAP equation with n_l active flavours.

The structure function in the massless scheme is:

$$\begin{aligned} F^{(n_l)}(Q^2, m_h^2) &= F^{(n_l)}(Q^2, 0) + O(\frac{m_h^2}{Q^2}) = \\ &= \sum_{i=q,\bar{q},g,h,\bar{h}} C_i^{(n_l+1)}\left(0, \alpha_s^{(n_l+1)}(Q^2)\right) \otimes f_i^{(n_l+1)}(Q^2) + O(\frac{m_h^2}{Q^2}) \end{aligned} \tag{3.13}$$

In this case, the divergences associated to the collinear emission of a heavy quarks are reabsorbed into the definition of the heavy quark PDF.

It is now possible to construct a matching relation for the PDFs at the matching scale μ_{match}:

$$f_i^{(n_l+1)}(\mu_{match}^2) = \sum_{j=q,\bar{q},g} K_{ij}\left(\frac{m_h^2}{Q^2}\right) \otimes f_j^{(n_l)}(\mu_{match}^2) \tag{3.14}$$

By inserting this equation in (3.13) we recover (3.12) up to power-suppressed contributions provided:

$$\sum_{q,\bar{q},g,h,\bar{h}} C_i^{(n_l+1)}(0) \otimes K_{ij}\left(\frac{m_h^2}{Q^2}\right) = C_j^{(n_l),0}\left(\frac{m_h^2}{Q^2}\right) \tag{3.15}$$

where $C_i^{(n_l),0}$ is the n_l coefficient function with all power suppressed terms set to zero. The matching condition can therefore be computed by calculating DIS structure functions in the massive and in the massless scheme and expanding the result order by order in (the same) α_s.

The K_{ij} terms are calculated as Operator Matrix Elements (OMEs) that appear in the operator product expansion of the commutator of two electromagnetic currents near the light cone. These OMEs are intrinsically related

to the heavy flavour coefficient functions computed in the asymptotic limit $Q^2 \gg m_h^2$. The basic idea when considering a theory with $(n_l + 1)$ massless partons and a single heavy flavour is reabsorbing the initial state collinear singularities into bare parton densities except for those that are regulated by the heavy quark mass. Instead of reabsorbing these terms into the parton densities as well, they are used to reconstruct the asymptotic behaviour of the heavy flavour coefficient functions through a *transition function* Γ_{ij}.

More precisely, the calculation of these terms starts from considering the heavy flavour contributions to a generic structure function $F(x, Q^2)$ in deep-inelastic scattering, in case of single electro-weak gauge-boson exchange at large virtualities Q^2. Structure functions are described as convolutions between the parton densities $f_i(x, \mu^2)$ and the Wilson coefficients $C_i^j(x, Q^2/\mu^2, m_h^2/\mu^2)$

$$F_j(x, Q^2) = \sum_i C_i^j \left(x, \frac{Q^2}{\mu^2}, \frac{m_h^2}{\mu^2} \right) \otimes f_i(x, \mu^2) \tag{3.16}$$

where the coefficient functions are calculable in perturbation theory and are the sum of both heavy H_i and light L_i contributions.

In the limit $Q^2 \gg m_h^2$, a generic heavy quark coefficient function H_i behave logarithmically as

$$H_i \left(x, \frac{Q^2}{\mu^2}, \frac{m_h^2}{\mu^2} \right) = \sum_{l=1}^{k} c_i^{(n,l)} \left(x, \frac{\mu^2}{m_h^2} \right) \log^l \frac{Q^2}{m_h^2} \tag{3.17}$$

where the above large logarithms arise when Q^2 is kept fixed and $m^2 \to 0$ so that they originate from collinear singularities. These collinear divergences can be removed via mass factorization. The key point is that a generic heavy flavour Wilson coefficient H_i factorize in the high-energy limit into a massive *transition function* and a light parton coefficient function, so that the asymptotic Wilson coefficients can be obtained starting from the massless contribution L_i only:

$$\begin{aligned} C_j^{\text{asymp}} &\left(x, n_l, \frac{Q^2}{\mu^2}, \frac{m_h^2}{\mu^2} \right) = \\ &\sum_i \Gamma_{ij} \left(x, \frac{m_h^2}{\mu^2} \right) \otimes L_i \left(x, n_l + 1, \frac{Q^2}{\mu^2} \right) + \mathcal{O}\left(\frac{m_h^2}{Q^2} \right) \end{aligned} \tag{3.18}$$

All the mass dependence is now transferred to the transition function Γ_{ij} and the removal of the logarithmic terms $\log^l(\mu^2/m_h^2)$ from the heavy flavour coefficient function leads to an enhancement by one of the number of light flavours n_l in the light parton coefficient functions. The transition function Γ_{ij} is process independent and contains all the mass dependence except for the power corrections of the form $\propto (m_h^2/Q^2)$. The dependence on the process is entirely included in the massless coefficient functions.

The transition function Γ_{ij} is formally equal to an *operator matrix element* (OME) K_{ij} that appears in the operator product expansion of the commutator of two electromagnetic currents near the lightcone. Suppressing the Lorentz index of the electromagnetic current, the expansion can be written as:

$$\lim_{z^2\to 0}[J(z), J(0)] = \sum_k \sum_m C_k^{(m)}(z^2) z_{\mu_1} ... z_{\mu_m} O_k^{\mu_1 ... \mu_m}(0) \tag{3.19}$$

where the coefficients $C_k^{(m)}(z^2)$ ($k = qg$) are the Fourier transforms of the light parton coefficient functions $L(Q^2/m_h^2)$ and m represents the spin of the local operator.

The OME K_{ij} obeys the expansion

$$K_{ij}\left(\frac{m_h^2}{\mu^2}\right) = \langle j|O_i|j\rangle = \delta_{ij} + \sum_{l=1}^{\infty} \alpha_s^l K_{ij}^{(l)} \tag{3.20}$$

of the twist-2 quark operators O_i between partonic states $|j\rangle$. They admit an expansion in the running coupling and they can be calculated in perturbative QCD. They describe Feynman diagrams in which an heavy flavour is produced starting from light quarks and gluons. At the moment, they are almost fully known up to α_s^3 [5, 6, 7, 8, 11, 12].

The calculation of these OMEs K_{ij} completely defines the matching relation for the PDFs when switching from a massive to a massless description. The matching relation for the PDFs (3.14) is the analogue of equation (3.7) for the coupling:

$$f_i^{(n_l+1)}(\mu_{match}^2) = \delta_{ij} f_j^{(n_l)}(\mu_{match}^2) + \Delta f_i \tag{3.21}$$

Also in this case, the first correction is proportional to $\log(\mu_{match}^2/m_h^2)$, which means that a matching performed at a scale equal to the heavy quark mass defines continuity in the PDFs at the first order when switching from the n_l to the $(n_l + 1)$ framework.

3.3 Perturbative and intrinsic heavy quark

The matching condition for the PDFs is usually obtained under the assumption of a fully perturbative heavy quark. Requiring a perturbative heavy flavour means that this quark is produced only via pair production starting from the light quarks and gluons. Under this hypothesis, the heavy flavour PDF can be expressed in terms of the light ones using equation (3.14), in which the index j explicitly runs only on light flavours and gluons. In fact, the requirement of a fully perturbative heavy quark can be expressed as follows:

$$f_h^{(n_l)}(x, \mu^2_{match}) = f_h^{(n_l)}(x, \mu^2_{match}) = 0 \tag{3.22}$$

This equation states that in the case of a perturbative heavy flavour the heavy quark (antiquark) PDF is completely determined by a perturbative evolution from a vanishing boundary condition at a scale of the order of the quark mass.

However, many models [21, 22] suggest the existence of an intrinsic (*i.e* non-perturbative) heavy component in the proton, especially in the case of the charm: the existence of an intrinsic heavy component in the nucleon is a rigorous prediction of QCD but an unambiguous experimental confirmation is still missing.

The interest in a possible intrinsic component of the charm PDF is determined by the fact that the charm has a mass $m_c \simeq 1.51$ GeV similar to the proton's: if we can surely neglect an intrinsic component of the bottom and the top, the intrinsic charm PDF could be significant.

The first suggestion of an intrinsic component of the charm PDF in the proton is due to Brodsky, Hoyer, Peterson, and Sakai (BHPS) in 1980 [21]: the BHPS prescription predicts an enhancement of the charm PDF in the large x region. In the BHPS model, one considers a non negligible five-quark Fock state $|uudQ\bar{Q}\rangle$ as the origin of an intrinsic contribution of the charm. The intrinsic charm PDF within a proton at a certain (unknown) scale in terms of the momentum fraction x can be computed, thus obtaining:

$$f_c(x) = f_{\bar{c}}(x) \propto x^2[6x(1+x)\log(x) + (1-x)(1+10x+x^2)] \tag{3.23}$$

which defines a bump of the charm content at $x \sim 0.2$.

This model suggests that the intrinsic sea quarks behave as *valencelike* quarks and then their distribution peaks at relatively large x. (By contrast, the extrinsic sea quarks are generated in the proton perturbatively through

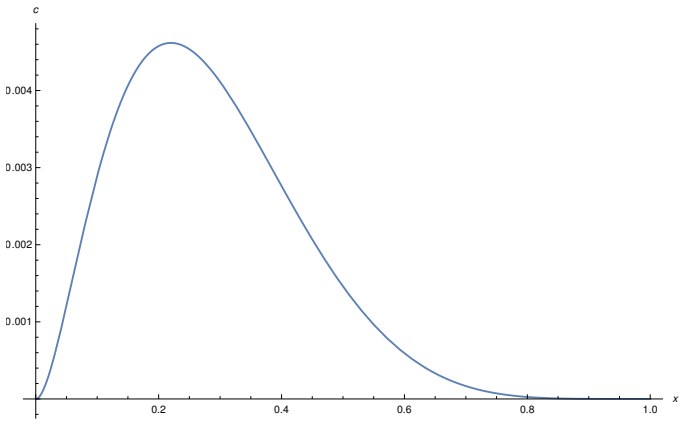

Figure 3.3: Intrinsic charm component of a proton using the BHPS prescription.

the splitting of gluons into quark-antiquark pairs in the DGLAP evolution, they dominate at very low parton momentum fraction x and so have a *sealike* features.)

Even if such intrinsic charm might have observable consequences at LHC at processes like γ+c [23] or open charm production [24], at the moment there is no an unambiguous confirmation of its existence and possible features.

If one wants to include an intrinsic heavy component in (3.14), equation (3.22) must be relaxed. The heavy PDF $f_h^{(n_l)}(x, \mu^2_{match})$ is thus non-zero and it must be introduced at all scales. As in the n_l scheme the heavy quark is treated as a massive object which decouples from the renormalization group equation, this PDF is scale independent.

3.4 Combining Massive and massless scheme

In the previous sections, we described how heavy flavours can be treated in a DIS process. Basically, one can perform calculations using a massive or a massless scheme. However, these frameworks are not accurate on the whole kinematic region, which naturally leads to the necessity of defining a General Mass Variable Flavour Number Scheme.

The construction of a GMVFS scheme must be performed with the main goal of defining a single framework in which both the FFNS and ZM-VFNS results are restored in the correct kinematic region. In other words, a GMVFNS must reproduce the massless scheme results in the high-energy region $Q^2 \gg$

m_h^2 and the massive scheme results when $Q^2 \sim m_h^2$. In order to perform this combination, corrections of order $\mathcal{O}(m_h^2/Q^2)$ that are neglected in the massless calculations must be restored.

Nowadays, different techniques are used in order to combine the massive and the massless scheme. The first method that was introduced [15] was only based upon a renormalization scheme with explicit heavy quark decoupling. This method - usually called ACOT after Aivazis, Collins, Olness and Tung - is based on the idea of calculating the coefficient functions by using standard massless collinear counterterms for massless partons, while massive collinear counterterms are used for heavy quarks. Several variants of this method were subsequently proposed, such as S-ACOT [16] and ACOT-χ [17].

In this thesis we study a somewhat different technique for the inclusion of heavy quark mass effects: the so-called Fixed-Order Next-Leading-Log FONLL scheme [1].

FONLL relies only on standard QCD factorization and calculations with massive quarks in the decoupling scheme and with massless quarks in the $\overline{MS}$ scheme. The FONLL method does not require novel factorization schemes as it is based on quantities calculated in well-defined schemes.

The original FONLL scheme is based on the observation that to obtain a description of physical quantities valid both at threshold and at high energy it is sufficient to add the n_l and $(n_l + 1)$ results and subtract the double counting: power corrections of $\mathcal{O}(m_h^2/Q^2)$ are restored in the massless calculation simply adding the massive fixed-order corrections. More precisely, the FONLL method is simply based on the idea of expanding out both the massless and massive schemes as power expansions in the strong coupling α_s and replacing the coefficients of the expansion in the former with their exact massive counterparts in the latter, when available. Any double counted term is then subtracted: they are constant and logarithmic terms that are both resummed in the massless scheme and explicitly present in the massive one. The final result has now a fixed order accuracy, thanks to the number of orders that have been included in perturbation theory (FO, fixed order) and a logarithmic accuracy ($\mathrm{N^kLL}$) due to the resummation of large logarithms in the massless scheme.

The name FONLL is historically related to the first application of this method to combine a fixed (second) order calculation with a next-to-leading log one. However this method is completely general and it can be used to combine a fixed order with a resummed calculation to any desired order.

In the next section we provide a detailed description of the FONLL

method explicitly applied to deep-inelastic structure functions. We consider the case of a perturbative heavy quark and we discuss how this hypothesis constrains the FONLL equations. We also discuss the possibility of introducing an *intrinsic* component of the heavy quark PDF, considering as a concrete example the interesting case of the charm.

Chapter 4

The FONLL method

In this section we analyse how to include heavy quarks contributions in deep-inelastic structure functions using the FONLL approach. This method was originally defined in the context of heavy quarks production in hadron collisions [19] and was then generalized to deep-inelastic scattering [1].

In this chapter we will theoretically describe the FONLL approach highlighting the main features of this method. We will explicitly show how the massless and the massive schemes can be combined together in order to obtain a single prescription that provides accurate results both at threshold $Q^2 \sim m_h^2$ and in the high-energy region $Q^2 \gg m_h^2$.

In this analysis, we consider the heavy flavour as a fully perturbative quark and we will discuss how the introduction of an intrinsic component of the heavy quark modifies the implementation of the FONLL method. As a concrete example, we will consider the case of a theory in which the charm quark is the single heavy flavour.

4.1 FONLL in deep-inelastic scattering

Let's consider a generic structure function $F(x, Q^2)$ and assume a single heavy quark with mass m_h.

In the massless scheme, which is accurate when $Q^2 \gg m_h^2$, the structure function reads:

$$F^{(n_l+1)}(x, Q^2) = x \int_x^1 \frac{dy}{y} \sum_{i=q,\bar{q},h,\bar{h},g} C_i^{(n_l+1)}\left(\frac{x}{y}, \alpha_s^{(n_l+1)}(Q^2)\right) f_i^{(n_l+1)}(y, Q^2) \tag{4.1}$$

where q is any light quark and h is the heavy quark. In this expression, the heavy quark is considered as a light parton. The coupling α_s and PDFs satisfy the standard evolution equation with $(n_l + 1)$ active flavours. The ZM coefficient functions $C_i^{(n_l+1)}$ at any given order k in α_s are obtained by setting explicitly $m_h = 0$ and the arising collinear singularities are subtracted in the $\overline{MS}$ scheme. This means that the logarithmic terms $\alpha_s ln(Q^2/m_h^2)$ are resummed up to N^kLL.

In the massive scheme, the same structure function can be written as:

$$F^{(n_l)}(x,Q^2) = x\int_x^1 \frac{dy}{y}\sum_{i=q,\bar{q},g} C_i^{(n_l)}\left(\frac{x}{y},\frac{Q^2}{m_h^2},\alpha_s^{(n_l)}(Q^2)\right) f_i^{(n_l)}(y,Q^2) \tag{4.2}$$

where the coefficient functions are computed retaining the mass dependence. This is a N^kLO fixed-order calculation. When $Q^2 \ll m_h^2$, the heavy quark mass drops out of the coefficient functions $C_i^{(n_l)}$ which then reduce to the standard massless $\overline{MS}$ scheme ones with n_l flavours.

The FONLL approach consists in replacing a finite number of massless terms with their massive counterparts, which requires to re-express both α_s and the PDFs in the massive scheme in terms of the massless ones. This must be done order by order in perturbation theory.

The massless and the massive scheme are perturbatively related by the equations defined in 3.2. At a fixed scale, the running coupling and the PDFs can be matched between the two schemes with the following equations:

$$\alpha_s^{(n_l+1)}(Q^2) = \alpha_s^{(n_l)}(Q^2) + \sum_{i=2}^{\infty} c_i(L)\times\left(\alpha_s^{(n_l)}(m_h^2)\right)^i \tag{4.3}$$

$$f_i^{(n_l+1)}(Q^2) = \int_x^1 \frac{dy}{y}\sum_{j=q,\bar{q},g} K_{ij}\left(\frac{x}{y},L,\alpha_s^{(n_l)}(Q^2)\right) f_j^{(n_l)}(y,Q^2) \tag{4.4}$$

where $i = q,\bar{q},g,h,\bar{h}$ and L is defined ad $L \equiv log\frac{Q^2}{m_h^2}$.

The matching relation for the running coupling is described in [2] while the matching for the PDFs is obtained in [4].

The matching functions K_{ij} can be expressed as a series in the running coupling

$$K_{ij}(Q^2) = \sum_n \alpha_s^n K_{ij}^n(Q^2) \tag{4.5}$$

and, at the moment, these terms are fully known up to α_s^2 [4] and most of them are analytically known at α_s^3 too [5, 6, 7, 8, 11, 12, 13].

In this section we discuss the FONLL method under the assumption of a fully perturbative heavy quark. The heavy quark is thus produced only from light quarks and gluons and the n_l heavy quark PDF satisfies the following relation:

$$f_h^{(n_l)}(x, m_h^2) = f_h^{(n_l+1)}(x, m_h^2) = 0 \tag{4.6}$$

This hypothesis imposes that the index j in equation (4.4) must be different from $h, \bar{h}$. For this reason, the first $2n_l + 1$ equations of (4.4) define the relations between the light quarks and gluon PDFs in the two schemes, while the last two equations provide the matching between the perturbative heavy quark and antiquark PDFs in the massless scheme and the light PDFs in the massive scheme.

In general, the matching between the n_l and (n_l+1) PDFs is performed at a fixed scale μ_{match} taken equal to the heavy quark mass m_h, as discussed in 3.2. Thanks to this choice, the matching conditions simplify because all the terms proportional to powers of $log(\mu_{match}/m_h)$ vanish: both the coupling and the PDFs are continuous at the first order if $\mu_{match}^2 = m_h^2$. This is no longer true at higher-orders.

The relation between the PDFs in the two schemes at a generic scale Q^2 can be obtained from the matching condition at a scale equal to m_h^2 simply applying the DGLAP evolution equation in the correct scheme.

Inverting the equations (4.3) and (4.4), $\alpha_s^{(n_l)}$ and $f_i^{(n_l)}$ can be expressed in terms of $\alpha_s^{(n_l+1)}$ and $f_i^{(n_l+1)}$. Plugging the result into (4.2), one obtains the expression for the massive structure function $F^{(n_l)}(x, Q^2)$ in terms of the coupling and the PDFs in the massless scheme:

$$F^{(n_l)}(x, Q^2) = x \int_x^1 \frac{dy}{y} \sum_{i=q,\bar{q},g} B_i\left(\frac{x}{y}, \frac{Q^2}{m_h^2}, \alpha_s^{(n_l+1)}(Q^2)\right) f_i^{(n_l+1)}(y, Q^2) \tag{4.7}$$

The coefficients B_i are such that substituting the matching (4.3) and (4.4) in the previous equation one gets back to the massive expression (4.2).

In order to match the two expressions for F in the massless scheme (4.1) and in the massive scheme (4.2), one can rewrite the massless structure function $F^{(n_l+1)}$ in terms of the light PDFs: using DGLAP evolution in absence of an intrinsic heavy quark, the heavy PDFs f_h and $f_{\bar{h}}$ can be expressed in terms of the light quark parton distributions $f_i^{(n_l+1)}$ convoluted with coefficient functions in a series of $\alpha_s^{(n_l+1)}$. It is now possible to rewrite the structure

function in the massless scheme only in terms of the light PDFs:

$$F^{(n_l+1)}(x,Q^2) = x\int_x^1 \frac{dy}{y}\sum_{i=q,\bar{q},g} A_i^{(n_l+1)}\left(\frac{x}{y},L,\alpha_s^{(n_l+1)}(Q^2)\right) f_i^{(n_l+1)}(y,Q^2) \tag{4.8}$$

At N^NLL, the coefficient functions $A_i^{(n_l+1)}$ are given by a perturbative expansion of the form

$$A_i^{(n_l+1)}(x,\alpha_s(Q^2,L) = \sum_{p=0}^{N}(\alpha_s^{(n_l+1)}(Q^2))^p \sum_{k=0}^{\infty} A_i^{p,k}(x)(\alpha_s^{(n_l+1)}(Q^2)L)^k \tag{4.9}$$

where the resummation of the logarithms is embedded in the infinite sum over k.

On the other hand, the coefficient functions B_i introduced in (4.7) admit a fixed order expansion:

$$B_i\left(x,\frac{Q^2}{m_h^2},\alpha_s^{(n_l+1)}(Q^2)\right) = \sum_{p=0}^{P}(\alpha_s^{(n_l+1)}(Q^2))^p B_i^p\left(x,\frac{Q^2}{m_h^2}\right) \tag{4.10}$$

where P denotes the order of accuracy.

Each of the perturbative contributions B_i^p can be expressed in a logarithmically enhanced part and a power suppressed part, which vanishes in the limit $Q^2 \gg m_h^2$. These terms can be thus decomposed:

$$B_i^p\left(x,\frac{Q^2}{m_h^2}\right) = B_i^{(0),p}\left(x,\frac{Q^2}{m_h^2}\right) + O\left(\frac{m_h^2}{Q^2}\right) \tag{4.11}$$

so that one can define the massless limit of B_i^p as:

$$B_i^p\left(x,\frac{Q^2}{m_h^2}\right) \underset{Q^2\gg m_h^2}{\longrightarrow} B_i^{(0),p}\left(x,\frac{Q^2}{m_h^2}\right) \tag{4.12}$$

In analogy with (4.10), one can define a perturbative expansion for the massless limit $B_i^{(0)}$:

$$B_i^0\left(x,\frac{Q^2}{m_h^2},\alpha_s^{(n_l+1)}(Q^2)\right) = \sum_{p=0}^{P}(\alpha_s^{(n_l+1)}(Q^2))^p B_i^{(0),p}\left(x,\frac{Q^2}{m_h^2}\right) \tag{4.13}$$

All the contributions in (4.10) which do not vanish in the limit $Q^2 \gg m_h^2$ must also be present in the coefficient functions in (4.9). These terms are exactly the coefficient functions defined in (4.11) so one can conclude that:

$$B_i^{(0),p}\left(x, \frac{Q^2}{m_h^2}\right) \equiv \sum_{k=0}^{p} A_i^{p-k,k}(x) L^k \tag{4.14}$$

This means that the massless limit of the coefficient functions B_i correspond to the logarithmic and constant terms which are present in (4.9).

In order to construct the FONLL structure function, we define the massless limit of the massive structure function $F^{(n_l,0)}$ as

$$F^{(n_l,0)}(x,Q^2) = x\int_x^1 \frac{dy}{y} \sum_{i=q,\bar{q},g} B_i^{(0)}\left(\frac{x}{y}, \frac{Q^2}{m_h^2}, \alpha_s^{(n_l+1)}(Q^2)\right) f_i^{(n_l+1)}(y,Q^2) \tag{4.15}$$

where the coefficient functions $B_i^{(0)}$ are defined in (4.13). Equation (4.15) contains terms which are present both in the massless and in the massive scheme, and thus must be subtracted in the final expression of the FONLL structure function.

The FONLL structure function can be obtained considering the massless structure function $F^{(n_l+1)}$ to which one subtracts the double counted terms $F^{(n_l,0)}$ and finally one replaces these terms with their exact massive contributions:

$$\begin{aligned} F^{FONLL}(x,Q^2) &= F^{(n_l)}(x,Q^2) + F^{(n_l+1)}(x,Q^2) - F^{(n_l,0)}(x,Q^2) = \\ &= F^{(n_l)}(x,Q^2) + F^{(d)}(x,Q^2) \end{aligned} \tag{4.16}$$

In the previous equation we introduced the *difference* term that is defined as:

$$F^{(d)}(x,Q^2) = F^{(n_l+1)}(x,Q^2) - F^{(n_l,0)}(x,Q^2) \tag{4.17}$$

At this point, one can observe that the FONLL method behaves properly in the two energy regimes $Q^2 \gg m_h^2$ and $Q^2 \sim m_h^2$: when $Q^2 \gg m_h^2$, equation (4.16) reproduces the massless scheme results, while for $Q^2 \sim m_h^2$ it describes the massive scheme plus the difference term (4.17) that is subleading.

In order to guarantee that (4.17) works properly, it is necessary to calculate $F^{(n_l+1)}$ at a power of α_s that is as high as that of $F^{(n_l)}$ at least: this way one subtracts terms that are really present in $F^{(n_l+1)}$. However, one can

generalizes (4.17) to the case in which $F^{(n_l)}$ is known with higher accuracy simply retaining in $F^{(n_l,0)}$ only those terms that are also present in $F^{(n_l+1)}$. In this case, it is no longer true that the FONLL result coincides with the massless scheme in the limit $Q^2 \gg m_h^2$ because $F^{(n_l)}$ and $F^{(n_l,0)}$ does not cancel anymore (some terms in $F^{(n_l,0)}$ have been excluded). In this energy region, the FONLL expression reduces to the massless scheme one up to mass suppressed terms.

4.1.1 Light and heavy contributions

Deep-inelastic structure functions are usually decomposed into a *heavy* and a *light* contribution. However, the definition of the heavy and light part is not unambiguous.

From the experimental point of view, a heavy structure function F_h^{exp} is defined as the one related to the production of a heavy quark in the final state, as this is indeed the only possible experimental definition. This is exactly the definition we assumed in 3.1.

Theoretically speaking, this definition is not suitable because of mass singularities. An explicit example is depicted in 4.1. The two diagrams are respectively a real and a virtual correction to the DIS process. The graph on the left contributes to F_h^{exp} because of the heavy quark in the final state, while the diagram on the right does not. The absence of the virtual correction in the calculation of F_h^{exp} can lead to singularities which would have cancelled including both real and virtual corrections.

An alternative definition is considering F_h as the contribution to the total structure function when all the charges are zero except for the heavy quark's. This way diagrams in 4.1 do not contribute to F_h: they are both included in the light structure function F_l [1], leading to a cancellation of potential singularities.

The decomposition of the structure function is now straightforward:

$$F(x, Q^2) = F_l(x, Q^2) + F_h(x, Q^2) \tag{4.18}$$

This equation leads to a separation of light and heavy contributions in the coefficient functions too:

$$C_i(x, \alpha_s(Q^2)) = C_{i,l}(x, \alpha_s(Q^2)) + C_{i,h}(x, \alpha_s(Q^2)) \tag{4.19}$$

[1] Given the definition of F_h, the complementary definition of F_l is straightforward: it is the contribution to the structure function setting to zero the charge of the heavy quark.

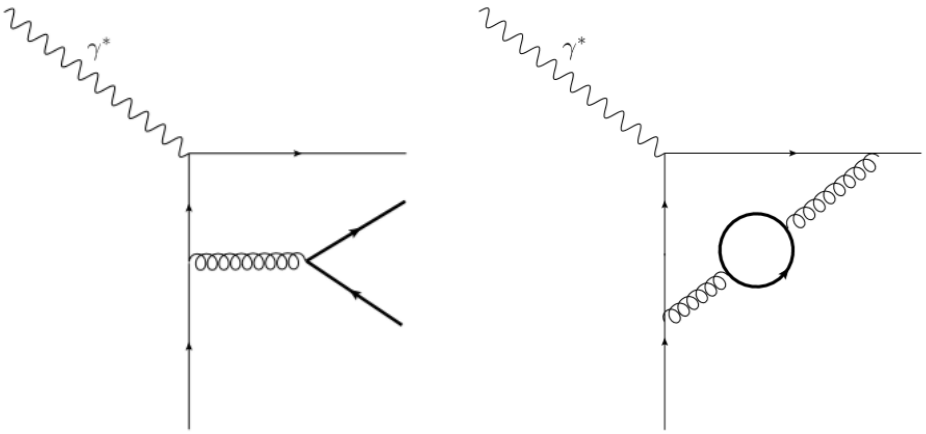

Figure 4.1: Explicit example of potential mass singularities: the picture on the left shows a diagram contributing to F_l and to $\widetilde{F_h}$. The diagram on the right contributes only to F_l.

where $C_{i,h}$ is defined as the contribution to C_i that is obtained when all the charges are zero but the heavy quark's.

In the case of an electromagnetic deep-inelastic scattering. the decomposition in light and heavy contributions defines which quark couples to the virtual incoming photon γ^*.

The same decomposition occurs for the FONLL expressions, so one can write:

$$F_l^{FONLL}(x,Q^2) = F_l^{(n_l)}(x,Q^2) + F_l^{(d)}(x,Q^2) \tag{4.20}$$

$$F_h^{FONLL}(x,Q^2) = F_h^{(n_l)}(x,Q^2) + F_h^{(d)}(x,Q^2) \tag{4.21}$$

4.1.2 Perturbative ordering

The perturbative ordering in matching the massless and the massive schemes for the computation of the FONLL structure functions can be defined in various ways. It is possible to combine the two schemes with an *absolute ordering*, order by order in α_s, or with a relative ordering, which means matching LO with LO, NLO with NLO, and so on. The issue is in general non-trivial because in a global parton fit one may want to combine data for observables whose LO starts at different orders in α_s.

The central point is that the leading order in the massless scheme differs from the leading order in the massive one in terms of power of the running coupling. For example, the leading order contribution to the heavy quark

production in the massless scheme is order $\mathcal{O}(\alpha_s^{(0)})$, while in the massive scheme is order $\mathcal{O}(\alpha_s)$. It it thus necessary to define how the matching between the two schemes is performed.

An advantage of the FONLL method is that the perturbative order at which heavy quark terms are included can be chosen freely. As we discussed at the end of section 4.1, if there is a mismatch in accuracy between the two schemes ($F^{(n_l)}$ has been computed with a higher accuracy than $F^{(n_l+1)}$), the FONLL structure function reproduces again the massless result in the high energy region up to higher order corrections.

As described in [1], up to α_s^2 one can define three different options for the perturbative matching:

- Scheme A: both $F^{(n_l)}$ and $F^{(n_l+1)}$ are calculated at order α_s, which means matching a LO calculation with a NLL one. There is no mismatch in accuracy between the two schemes.

- Scheme B: different accuracy in α_s but same relative ordering in the computation of the different contributions to the FONLL structure functions. $F^{(n_l)}$ is computed at NLO, which is $\mathcal{O}(\alpha_s^2)$, while $F^{(n_l+1)}$ is computed again at NLL, $\mathcal{O}(\alpha_s)$. In this case the massive expression exceeds in accuracy the massless one when L is not large. Thus, as previously described, in the definition of $F^{(n_l,0)}$ we must retain only terms which are present in $F^{(n_l+1)}$ too.

- Scheme C: the same as scheme A but one order higher. $F^{(n_l)}$ is computed at NLO, $\mathcal{O}(\alpha_s^2)$, while $F^{(n_l+1)}$ is computed at NNLL, $\mathcal{O}(\alpha_s^2)$.

The same idea can be applied also to higher-order matching. In the next chapter we will calculate explicit FONLL expressions at $\mathcal{O}(\alpha_s^3)$, performing the matching using the analogue of scheme A/C at this order: all the equations will be expanded up to α_s^3.

4.2 Heavy quark PDF: the charm

Among heavy quarks, the charm plays an important role because it has a mass close to the scale where one would expect the non perturbative behaviour to manifest. For this reason, the assumption for a fully perturbative heavy quark may be unsatisfactory when considering the charm quark.

The FONLL method has been improved in order to take into account the possibility for an intrinsic component of the heavy quark PDF. Equation (4.6) is relaxed and $f_h^{(n_l+1)}(x, m_h^2) = f_{\bar{h}}^{(n_l+1)}(x, m_h^2)$ is just given by some parametrization, with parameters to be determined by comparing to experimental data. Considering both an intrinsic and a perturbative component of the heavy quark leads to new contributions to the structure functions: as an example, the heavy structure function $F_h^{(n_l)}$ now receive a contribution from $f_h^{(n_l)}$ and $f_{\bar{h}}^{(n_l)}$ which starts at $\mathcal{O}(\alpha_s^0)$ (i.e. at the parton model level).

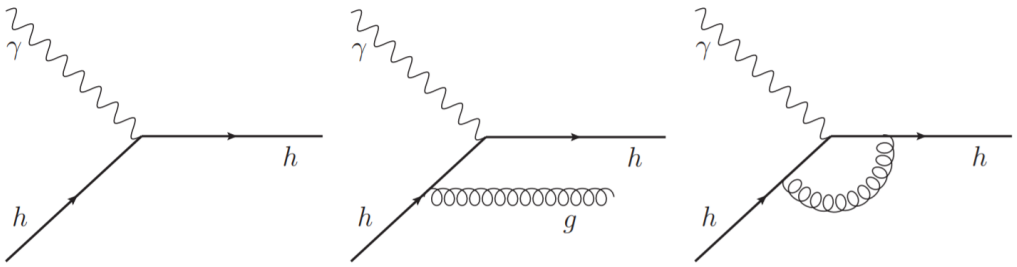

Figure 4.2: Feynman diagrams representing the contributions to the heavy $F_h^{(n_l)}(x, Q^2)$ structure function induced by the heavy quark PDF. From left to right, the LO diagram and the NLO real and virtual diagrams are shown.

A complete implementation of the FONLL equations with the inclusion of an intrinsic component of the heavy quark up to α_s^2 can be found in [25].

Even if considering both a perturbative and an intrinsic part of the heavy quark PDF can surely improve the FONLL method, in this thesis we will not consider an intrinsic component of the heavy quark: in the next chapter, we will explicitly construct the FONLL structure functions at $\mathcal{O}(\alpha_s^3)$ with a perturbative heavy flavour.

At the moment, the matching condition for the charm PDF is performed at α_s^2. Figure 4.3 shows a comparison between a fully perturbative charm obtained with a α_s^2 matching and a *fitted* charm. A *fitted* heavy quark is obtained performing a fit along with light quarks and gluon PDFs starting from a proper parametrization. In this way, the fitted charm does not make any distinction between a perturbative and an intrinsic component and whether or not its PDF vanishes and at what scale is answered by the fit.

In figure 4.3 the scale is equal to the pole mass of the charm, $m_c = 1.51\text{GeV}$. If one performs a matching at a scale equal to the charm mass, it must be underlined that this mass is known with low accuracy.

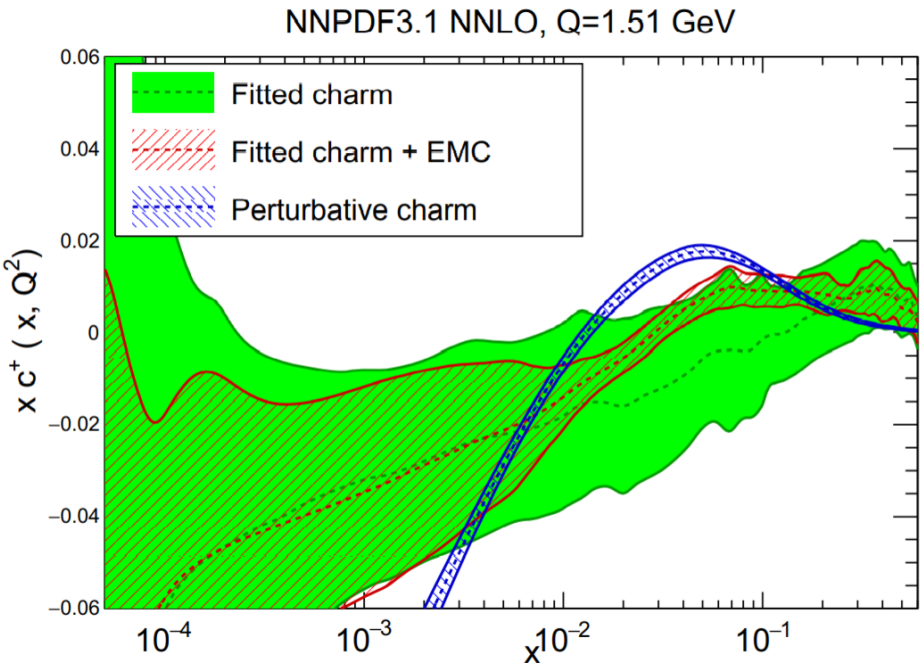

Figure 4.3: Comparison between a perturbative charm up to a α_s^2 matching and a fitted charm. The *fitted charm + EMC* curve includes data from the European Muon Collaboration experiment of deep-inelastic scattering with muon beams. This experiment was particularly sensitive to the charm PDF at large x but the data analysis is rather controversial: in the standard fitted charm PDF, EMC data are not included.

On the one hand, the fitted charm shows a bump in the large x region, that is probably associated to the intrinsic component, and a slow decrease at small x. The fitted charm has a large error bar in the whole domain. On the other hand, the perturbative charm does not show any peak in the large x region and it has a very different shape than the fitted quark.

At this point, one can notice that the matching condition for the charm PDF at $\mathcal{O}(\alpha_s^2)$ is:

$$f_h^{(n_l+1)}(x, m_h^2) = \alpha_s^2 \int \frac{dz}{z} \sum_{j=q,\bar{q},g} K_{hj}(z) f_j^{(n_l)}(\frac{x}{z}, m_h^2) + \mathcal{O}(\alpha_s^3) \tag{4.22}$$

This equation is obtained from the general matching condition (4.4) with the assumption of a perturbative heavy quark, $f_h^{(n_l)}(x, m_h^2) = 0$, and observing that the linear term is zero if $Q^2 = m_h^2$. Equation (4.22) shows that the α_s^2

matching is concretely the leading order contribution: the real shape of the charm PDF can be very different than the one depicted in figure 4.3.

The motivation for considering a fully perturbative heavy quark PDF up to α_s^3 is now straightforward: a perturbative heavy flavour PDF is described in terms of light quarks and gluon PDFs starting at $\mathcal{O}(\alpha_s^2)$, which means that the $\mathcal{O}(\alpha_s^3)$ contributions are the first non trivial corrections to the leading order. A comparison between a perturbative charm at α_s^3 and a fitted charm can clarify if a higher-order matching for the heavy quark provide a better description of its PDF or if a fitted charm is the best option for studying the charm content of the proton, even with a significant error. Furthermore, this comparison can be useful in a first estimation of the intrinsic charm contribution. We expect a peak at $x \sim 0.2$ as a manifestation of the intrinsic charm: if a α_s^3 charm shows an increase in the same region, we can conclude that part of the peak we explicitly observe in the fitted charm is due to the perturbative contribution.

Chapter 5

FONLL method up to $\mathrm{O}(\alpha_{\mathrm{S}}^3)$

5.1 Motivation

In this chapter we provide explicit expressions of the FONLL equations for deep-inelastic electromagnetic structure functions at $\mathcal{O}(\alpha_s^3)$. Before this work, the FONLL equations were fully known and commonly used up to the second order in the strong coupling: in this thesis we present the FONLL structure functions using the perturbative ordering defined as *scheme C* in 4.1.2 one order higher.

The importance of computing the FONLL equations at $\mathcal{O}(\alpha_s^3)$ is determined by the necessity of high precision predictions in perturbative QCD. In the context of strong interactions, accuracy is usually achieved by computing calculations that include an increasing number of terms of the perturbative expansion in the strong coupling. Nowadays leading-order cross sections in QCD can be computed for an arbitrary number of external particles. Automation has been achieved in recent years also for NLO calculations and an increasing number of NNLO calculations is now available in computer programs. Moreover, for simple hadron-collider processes, different calculations have achieved a $\mathrm{N^3LO}$ accuracy [38, 39]. The recent $\mathrm{N^3LO}$ computation [20] of the partonic cross section for the production of a Higgs boson via the fusion of two bottom quarks showed that $\mathrm{N^3LO}$ is surely the new frontier for high-precision predictions.

In particular, precise theoretical predictions for LHC processes require precise and reliable parton distribution functions, which are usually investigated through DIS processes. Several ingredients are either already available,

or focus of current research. For instance, deep-inelastic scattering coefficient functions with massless quarks have been known at three loops for a long time [40], and a lot of progress has been done in the context of heavy quarks [5, 6, 7, 8, 11, 12, 13]. A detailed study of the matching condition for the charm PDF at α_s^3 can provide important phenomenological result as the first non trivial correction to the leading order contribution.

This chapter is structured as follows: in the first section we provide analytic expressions for the FONLL structure functions up to $\mathcal{O}(\alpha_s^3)$ describing the matching conditions for the running coupling and the PDFs, and then explicitly constructing the FONLL structure functions as shown in 4.1. In this first section we describe the complete theoretical framework without providing any numerical results: as we will see, not all the massive Wilson coefficients that are required are fully known at α_s^3.

The second part concerns the heavy quark PDF: we will study the perturbative matching condition of the charm PDF at α_s^3, describing in detail our numerical implementation and providing a numerical result. Our result will be then compared to the plot 4.3, analysing the differences between our result, a two-loop matching charm and a fitted charm.

5.2 Explicit implementation

In this section we provide explicit expressions for the FONLL electromagnetic deep-inelastic structure functions up to $\mathcal{O}(\alpha_s^3)$. In this analysis we use the same notation as [1]. First of all, we discuss how to switch between the massive and the massless scheme defining the matching conditions for the running coupling and the PDFs between the two frameworks. Following the idea described in the previous chapter, we then obtain the FONLL structure functions expanding out the massless equations and substituting a finite number of terms with their massive counterparts. These same equations up to $\mathcal{O}(\alpha_s^2)$ are explicitly described in [1].

5.2.1 Matching conditions

The relation between α_s in the massive and in the massless schemes at a generic scale Q^2 is obtained in [2] comparing an effective n_l flavour theory

with a full $(n_l + 1)$ flavour theory:

$$\frac{\alpha_s^{(n_l+1)}(Q^2)}{\pi} = \frac{\alpha_s^{(n_l)}(Q^2)}{\pi} + \left(\frac{\alpha_s^{(n_l)}(Q^2)}{\pi}\right)^2 \frac{T_R L}{3} + \\ + \left(\frac{\alpha_s^{(n_l)}(Q^2)}{\pi}\right)^3 \left[\frac{T_R^2}{9}L^2 + \frac{5C_A T_R - 3C_F T_R}{12}L + \frac{13}{48}T_R C_F + \right. \\ \left. - \frac{2}{9}T_R C_A\right] + \mathcal{O}(\alpha_s^4) \tag{5.1}$$

where we used the common notation $T_R = 1/2$ for the trace normalization of the fundamental representation , $C_A = 3$ for the normalization of the Casimir operators in the adjoint representation, $C_F = 4/3$ for the normalization of the Casimir operators in the fundamental representation and we defined $L = log(\frac{Q^2}{m_h^2})$. The mass m_h is the heavy quark mass in the $\overline{MS}$ scheme at a scale Q^2.

It is easy to understand the origin of the different terms in (5.1) considering the self-energy contribution to the gluon propagator. For example, the first correction is proportional to $\frac{T_R L}{3}$, which is related to the difference in β_0 - the first coefficient of the β-function - in the two theories. In fact, β_0 is proportional to the number of flavours through:

$$\beta_0 \sim \frac{T_R n_f}{3} \tag{5.2}$$

When considering a one loop approximation, the number of active flavours which enter the loop is different in the two schemes.

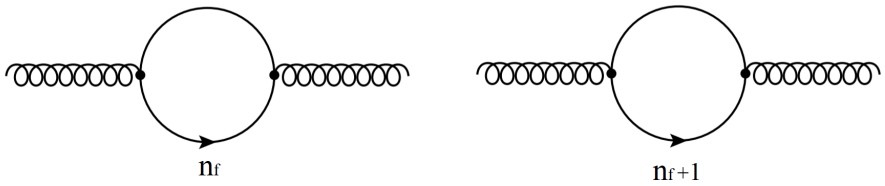

Figure 5.1: Contribution to the β-function in the one loop approximation with different numbers of active flavours in the loop.

The difference is thus $\delta\beta_0 = T_R/3$. This term is associated to a logarithmic contribution L explicitly dependent on the $(n_l + 1)$-th flavour mass.

One order higher, the calculation involves both a propagator with two contributions one-particle irreducible and graphs with internal corrections in the loop (for example, a gluon can be exchanged between the fermion lines). The first contribution gives raise to a term proportional to $(\delta\beta_0)^2 = \frac{T_R^2}{9}$ while the second contribution leads to all the other terms in (5.1), where a mixture of terms proportional to C_A and C_F arise. At this order, the calculation leads to contributions proportional to L^2, L and L^0. This same strategy can be applied order by order i perturbation theory for matching the coupling in the two schemes at any desired order.

It is now convenient to redefine the coupling as

$$\widetilde{\alpha_s}(Q^2) \equiv \frac{\alpha_s(Q^2)}{2\pi} \tag{5.3}$$

and, for simplicity, we will omit the tilde symbol from now on. With this definition and substituting the colour factors C_A and C_F with their values, equation (5.1) becomes:

$$\begin{aligned}\alpha_s^{(n_l+1)}(Q^2) = \alpha_s^{(n_l)}(Q^2) + {\alpha_s^{(n_l)}}^2(Q^2)\frac{2T_R L}{3} + \\ + {\alpha_s^{(n_l)}}^3(Q^2)\left[\frac{4}{9}T_R^2 L^2 + \frac{11}{3}T_R L - \frac{11}{9}T_R\right] + \mathcal{O}(\alpha_s^4)\end{aligned} \tag{5.4}$$

The matching condition at the scale $Q^2 = m_h^2$ is: [1]

$$\alpha_s^{(n_l+1)}(m_h^2) = \alpha_s^{(n_l)}(m_h^2) - \frac{11}{9}T_R{\alpha_s^{(n_l)}}^3(m_h^2) + \mathcal{O}(\alpha_s^4) \tag{5.5}$$

Finding the relation between $\alpha_s(Q^2)$ and $\alpha_s(m_h^2)$ requires solving the renormalization group equation RGE, expanding the β-function at the desired order:

$$L = \int_{\alpha_s(m_h^2)}^{\alpha_s(Q^2)} d\alpha \frac{1}{-\beta_0\alpha^2 + \beta_1\alpha^3 + \beta_2\alpha^4} \tag{5.6}$$

[1] In this analysis we considered the heavy mass in the $\overline{MS}$ scheme. For simplicity, in the next section we will explicitly consider the matching condition for the heavy quark PDF at a scale equal to the pole mass of the charm. The $\overline{MS}$ mass m_h and the pole mass M are related though a perturbative expansion [45]. One can thus obtain the matching relation at a scale equal to the pole mass of the heavy quark:

$$\alpha_s^{(n_l+1)}(M^2) = \alpha_s^{(n_l)}(M^2) + \frac{7T_R}{3}{\alpha_s^{(n_l)}}^3(M^2).$$

The only difference with (5.5) is the coefficient of α_s^3.

where the coefficients β_i in a theory with n_f active flavours are defined as:

$$\begin{aligned}\beta_0 &= \frac{33 - 4T_R n_f}{6} \\ \beta_1 &= \frac{153 - 38T_R n_f}{24} \\ \beta_2 &= \frac{2857}{16} - \frac{5033 T_R n_f}{72} + \frac{325 {T_R}^2 {n_f}^2}{108}\end{aligned} \tag{5.7}$$

Solving iteratively equation (5.6), one finds the following relation, which expresses how the running coupling evolves from a starting scale m_h^2 to a generic scale Q^2:

$$\begin{aligned}\alpha_s(Q^2) = \alpha_s(m_h^2)\Bigg[1 - \beta_0\alpha_s(m_h^2)L + \alpha_s^2(m_h^2)\bigg(\beta_0^2 L^2 + \beta_1 L\bigg) + \\ + \alpha_s^3(m_h^2)\bigg(-\beta_0^3 L^3 - \frac{5}{2}\beta_1\beta_0 L^2 + \beta_2 L\bigg)\Bigg] + \mathcal{O}(\alpha_s^5(m_h^2))\end{aligned} \tag{5.8}$$

At this point the matching conditions for the running coupling are complete. In order to construct the FONLL equations, the same procedure must be applied to the PDFs.

Studying the matching conditions for the PDFs requires the same calculations performed for the matching of the running coupling. First of all, we can calculate how a PDF $f(x, \mathrm{Q}^2)$ evolves from a starting scale m_h^2 to a generic scale Q^2 using the DGLAP equation. For simplicity, this calculation can be performed in Mellin space, where a convolution becomes a simple product and then we can turn back to x-space. We thus need to solve the following equation

$$\int_{f(N,m_h^2)}^{f(N,Q^2)} \frac{df(N,Q^2)}{f(N,Q^2)} = \int_{\alpha_s(m_h^2)}^{\alpha_s(Q^2)} d\alpha \frac{\gamma^0\alpha + \gamma^1\alpha^2 + \gamma^2\alpha^3}{-\beta_0\alpha^2 + \beta_1\alpha^3 + \beta_2\alpha^4} \tag{5.9}$$

where $\gamma^n = \gamma_{ij}^n$ defines the coefficients of the anomalous dimension γ_{ij} [26], which is the Mellin transform of the splitting function P_{ij}.

The solution up to third order in α_s in x-space is given by:

$$
\begin{aligned}
f_i^{(n_l)}(x,Q^2) = f_i^{(n_l)}(x,m_h^2) + \alpha_s^{(n_l)} \int_x^1 \frac{dz}{z} \sum_j P_{ij}^{(n_l),0}(z) f_j^{(n_l)}(\frac{x}{z},m_h^2) L + \\
+\alpha_s^{(n_l)^2} \Bigg[-\frac{1}{2}\beta_0^{(n_l)} \int_x^1 \frac{dz}{z} \sum_j P_{ij}^{(n_l),0}(z) f_j^{(n_l)}(\frac{x}{z},m_h^2) L^2 + \\
+ \frac{1}{2} \int_x^1 \frac{dz}{z} \sum_j \left(P^{(n_l),0} \otimes P^{(n_l),0} \right)_{ij} (z) f_j^{(n_l)}(\frac{x}{z},m_h^2) L^2 + \\
+ \int_x^1 \sum_j P_{ij}^{(n_l),1}(z) f_j^{(n_l)}(\frac{x}{z},m_h^2) L \Bigg] + \\
+\alpha_s^{(n_l)^3} \Bigg[\frac{1}{6} \int_x^1 \frac{dz}{z} \sum_j \left(P^{(n_l),0} \otimes P^{(n_l),0} \otimes P^{(n_l),0} \right)_{ij} (z) f_j^{(n_l)}(\frac{x}{z},m_h^2) L^3 + \\
+ \frac{1}{2}\beta_1^{(n_l)} \int_x^1 \frac{dz}{z} \sum_j P_{ij}^{(n_l),0}(z) f_j^{(n_l)}(\frac{x}{z},m_h^2) L^2 + \\
- \frac{1}{2}\beta_0^{(n_l)} \int_x^1 \frac{dz}{z} \sum_j \left(P^{(n_l),0} \otimes P^{(n_l),0} \right)_{ij} (z) f_j^{(n_l)}(\frac{x}{z},m_h^2) L^3 + \\
+ \frac{1}{3}\beta_0^{(n_l)^2} \int_x^1 \frac{dz}{z} \sum_j P_{ij}^{(n_l),0}(z) f_j^{(n_l)}(\frac{x}{z},m_h^2) L^3 + \\
- \beta_0^{(n_l)} \int_x^1 \frac{dz}{z} \sum_j P_{ij}^{(n_l),1}(z) f_{ij}^{(n_l)}(\frac{x}{z},m_h^2) L^2 + \\
+ \int_x^1 \frac{dz}{z} \sum_j \left(P^{(n_l),0} \otimes P^{(n_l),1} \right)_{ij} (z) f_j^{(n_l)}(\frac{x}{z},m_h^2) L^2 + \\
+ \int_x^1 \frac{dz}{z} \sum_j P_{ij}^{(n_l),2}(z) f_j^{(n_l)}(\frac{x}{z},m_h^2) L \Bigg]
\end{aligned}
\tag{5.10}
$$

where we used the shorthand notation $\alpha_s = \alpha_s(m_h^2)$ and the indexes run on gluon and quarks: $i,j = q,\bar{q},g$. The main differences between the α_s^2 and the α_s^3 solutions are due to the change in the running coupling (5.8), the third iteration of the splitting function P_{ij}^0, a mixed contribution between the α_s and α_s^2 terms and the appearance of the next-to-next-to-leading order splitting functions P_{ij}^2.

The matching conditions between the PDFs in the two schemes are described in equations (4.4): at a scale equal to the heavy quark mass, for the

light quarks and the gluon the following equation is valid:

$$f_i^{(n_l+1)}(x,m_h^2) = f_i^{(n_l)}(x,m_h^2) + \alpha_s^2 \int \frac{dz}{z} \sum_{j=q,\bar{q},g} K_{ij}(z) f_j^{(n_l)}(\frac{x}{z},m_h^2) + \\ + \alpha_s^3 \int \frac{dz}{z} \sum_{j=q,\bar{q},g} K_{ij}^1(z) f_j^{(n_l)}(\frac{x}{z},m_h^2) + \mathcal{O}(\alpha_s^4) \tag{5.11}$$

In the absence of an intrinsic heavy contribution, the heavy quark PDF satisfies the constraint:

$$f_h^{(n_l)}(x,m_h^2) = f_{\bar{h}}^{(n_l)}(x,m_h^2) = 0 \tag{5.12}$$

and thus its matching condition becomes:

$$f_h^{(n_l+1)}(x,m_h^2) = f_{\bar{h}}^{(n_l+1)}(x,m_h^2) = \alpha_s^2 \int \frac{dz}{z} \sum_{j=q,\bar{q},g} K_{hj}(z) f_j^{(n_l)}(\frac{x}{z},m_h^2) + \\ + \alpha_s^3 \int \frac{dz}{z} \sum_{j=q,\bar{q},g} K_{hj}^1(z) f_j^{(n_l)}(\frac{x}{z},m_h^2) + \mathcal{O}(\alpha_s^4) \tag{5.13}$$

The heavy quark PDF starts at order α_s^2.

The perturbative coefficients K_{ij} are calculated as described in section 3.2. Up to α_s^2 they are calculated in [4] while at α_s^3 they are defined in [5], [6], [7] and [8] for the light quarks and gluons and in [11], [12] and [13] for the heavy contribution. Not all the cited three-loop matching contributions are fully known.

We can now obtain the matching condition for the PDFs at a generic scale Q^2. As for the gluon PDF, the coefficient functions start at order α_s: we can thus truncate the relation at $\mathcal{O}(\alpha_s^2)$, obtaining:

$$f_g^{(n_l)}(x,Q^2) = f_g^{(n_l+1)}(x,Q^2) + \alpha_s L \frac{2T_R}{3} f_g^{(n_l+1)}(x,m_h^2) + \\ - \alpha_s^2 \int_x^1 \frac{dz}{z} \sum_j K_{gj}(z) f_j^{(n_l+1)}(\frac{x}{z},m_h^2) - \alpha_s^2 \frac{L^2}{2} \beta_0^{(n_l)} \frac{2T_R}{3} f_g^{(n_l+1)}(x,m_h^2) + \\ + \alpha_s^2 \frac{2T_R}{3} \frac{L^2}{2} \int_x^1 \frac{dz}{z} P_{gg}^{(n_l),0}(z) f_g^{(n_l+1)}(\frac{x}{z},m_h^2) + \\ - \alpha_s^2 L \int_x^1 \frac{dz}{z} \sum_j \left[P_{gj}^{(n_l+1),1} - P_{gj}^{(n_l),1} \right](z) f_j^{(n_l+1)}(\frac{x}{z},m_h^2) + \mathcal{O}(\alpha_s^3) \tag{5.14}$$

For the light quarks a complete expansion up to $\mathcal{O}(\alpha_s^3)$ is needed.

$$
\begin{aligned}
f_q^{(n_l)}(x,Q^2) &= f_q^{(n_l+1)}(x,Q^2) - \alpha_s^2\Bigg[\int_x^1 \frac{dz}{z}\sum_j K_{qj}(z) f_j^{(n_l+1)}(\frac{x}{z},m_h^2)+ \\
&- \frac{2T_R}{3}\frac{L^2}{2}\int_x^1 \frac{dz}{z}\sum_{j=q,\bar{q}} P_{qj}^{(n_l),0}(z) f_j^{(n_l+1)}(\frac{x}{z},m_h^2)+ \\
&- L\int_x^1 \frac{dz}{z}\Big(-\Delta_{qq}(z)\Big) f_q^{(n_l+1)}(\frac{x}{z},m_h^2)\Bigg] - {\alpha_s}^3\Bigg[\int_x^1 \frac{dz}{z}\sum_j K_{qj}^1(z) f_j^{(n_l+1)}(\frac{x}{z},m_h^2)+ \\
&+ L\int_x^1 \frac{dz}{z}\sum_j \Big(P^{(n_l),0}\otimes K\Big)_{qj}(z) f_j^{(n_l+1)})(\frac{x}{z},m_h^2)+ \\
&\frac{1}{6}\int_x^1 \frac{dz}{z}\sum_j \Big((P^0\otimes P^0\otimes P^0)_{qj}^{(n_l+1)} - (P^0\otimes P^0\otimes P^0)_{qj}^{(n_l)}\Big)(z) f_j^{(n_l+1)}(\frac{x}{z},m_h^2)L^3+ \\
&- \frac{11T_R}{9}L\int_x^1 \frac{dz}{z}\sum_j P_{qj}^{(n_l),0}(z) f_j^{(n_l+1)}(\frac{x}{z},m_h^2)+ \\
&+ \frac{L^2}{2}\frac{19T_R}{3}\int_x^1 \sum_j P_{qj}^{(n_l),0}(z) f_j^{(n_l+1)}(\frac{x}{z},m_h^2)+ \\
&- \frac{L^3}{2}\beta_0^{(n_l+1)}\int_x^1 \sum_j (P^0\otimes P^0)_{qj}^{(n_l+1)}(z) f_j^{(n_l+1)}(\frac{x}{z},m_h^2)+ \\
&+ \frac{L^3}{2}\beta_0^{(n_l)}\int_x^1 \sum_j (P^0\otimes P^0)_{qj}^{(n_l)}(z) f_j^{(n_l+1)}(\frac{x}{z},m_h^2)+ \\
&+ \frac{L^3}{3}\big(\beta_0^{(n_l+1)^2} - \beta_0^{(n_l)^2}\big)\int_x^1 \frac{dz}{z}\sum_j P_{qj}^{(n_l),0}(z) f_j^{(n_l+1)}(\frac{x}{z},m_h^2)+ \\
&- \beta_0^{(n_l)}L^2\int_x^1 \sum_j \big[P^{(n_l+1),1} - P^{(n_l),1}\big]_{qj}(z) f_j^{(n_l+1)}(\frac{x}{z},m_h^2)+ \\
&+ \frac{2T_R}{3}L^2\int_x^1 \sum_j P_{qj}^{(n_l+1),1}(z) f_j^{(n_l+1)}(\frac{x}{z},m_h^2)+ \\
&+ L^2\int_x^1 \sum_j \big[(P^0\otimes P^1)^{(n_l+1)} - (P^0\otimes P^1)^{(n_l)}\big]_{qj}(z) f_j^{(n_l+1)}(\frac{x}{z},m_h^2)+ \\
&+ L\int_x^1 \sum_j \big[P_{qj}^{(n_l+1),2} - P_{qj}^{(n_l),2}\big](z) f_j^{(n_l+1)}(\frac{x}{z},m_h^2)\Bigg]
\end{aligned}
\tag{5.15}
$$

Using the same notation as [1], we defined $\Delta_{qq}(z)$ starting from:

$$P_{qj}^{(n_l+1),1}(z) - P_{qj}^{(n_l),1}(z) = -\delta_{jq}\Delta_{qq}(z) \tag{5.16}$$

so that

$$\Delta_{qq}(z) = C_F T_R \left[\frac{1+z^2}{1-z}\left(\frac{2}{3}\log(z) + \frac{10}{9}\right) + \frac{4}{3}(1-z)\right]_+ \tag{5.17}$$

Most of the multiple convolutions obtained in (5.15) are explicitly computed in [9] and [10].

5.2.2 Structure functions

In this section we will show how to construct the FONLL structure functions at $\mathcal{O}(\alpha_s^3)$. In the previous chapter we defined the massive structure function as follows:

$$F^{(n_l)}(x,Q^2) = x\int_x^1 \frac{dy}{y}\sum_{i=q,\bar{q},g} C_i^{(n_l)}\left(\frac{x}{y}, \frac{Q^2}{m_h^2}, \alpha_s^{(n_l)}(Q^2)\right) f_i^{(n_l)}(y,Q^2) \tag{5.18}$$

The FONLL method requires to express the previous equation in terms of the coupling and the PDFs in the massless scheme, obtaining a structure function of the form:

$$F^{(n_l)}(x,Q^2) = x\int_x^1 \frac{dy}{y}\sum_{i=q,\bar{q},g} B_i\left(\frac{x}{y}, \frac{Q^2}{m_h^2}, \alpha_s^{(n_l+1)}(Q^2)\right) f_i^{(n_l+1)}(y,Q^2) \tag{5.19}$$

Expanding out both the coefficient functions C_i and B_i in terms of α_s in the two schemes one obtains the following perturbative expansions:

$$C_i^{(n_l)} = \sum_{p=0}^{P}\left(\alpha_s^{(n_l)}(Q^2)\right)^p C_i^p \qquad B_i = \sum_{p=0}^{P}\left(\alpha_s^{(n_l+1)}(Q^2)\right)^p B_i^p \tag{5.20}$$

At this point we can explicitly separate the light and heavy contributions to the total structure function and the coefficient functions:

$$\begin{aligned} F(x,Q^2) =& F_l(x,Q^2) + F_h(x,Q^2) \\ C_i(x,\alpha_s(Q^2)) =& C_{i,l}(x,\alpha_s(Q^2)) + C_{i,h}(x,\alpha_s(Q^2)) \end{aligned}$$

The coefficients B_i can be found rewriting the coefficient functions $C_i^{(n_l)}$ in terms of $\alpha_s^{(n_l+1)}$ at a generic scale Q^2 using (5.4) and the $f_i^{(n_l)}$ in terms of $f_i^{(n_l+1)}$ using (5.14) and (5.15).

As for the running coupling, it is necessary to express $\alpha_s^{(n_l)}(Q^2)$ as an expansion of $\alpha_s^{(n_l+1)}(Q^2)$. Inverting equation (5.4) one finds:

$$\alpha_s^{(n_l)}(Q^2) = \alpha_s^{(n_l+1)}(Q^2) - \frac{2}{3}T_R L \alpha_s^{(n_l+1)^2}(Q^2) + \tag{5.21}$$

$$- \alpha_s^{(n_l+1)^3}(Q^2)\left[- \frac{4}{9}T_R^2 L^2 + \frac{11}{3}T_R L - \frac{11}{9}T_R \right] \tag{5.22}$$

Up to the third order in α_s, $C_i^{(n_l)}$ can thus be written as:

$$\begin{aligned}
&C_i^{(n_l)} = C_i^{(n_l),0} + \alpha_s^{(n_l)}(Q^2) C_i^{(n_l),1} + \alpha_s^{(n_l)^2}(Q^2) C_i^{(n_l),2} + \alpha_s^{(n_l)^3}(Q^2) C_i^{(n_l),3} = \\
&= C_i^{(n_l),0} + \left[\alpha_s^{(n_l+1)}(Q^2) - \frac{2}{3}T_R L \alpha_s^{(n_l+1)^2}(Q^2) + \right. \\
&\left. - \alpha_s^{(n_l+1)^3}(Q^2)\left(- \frac{4}{9}T_R^2 L^2 + \frac{11}{3}T_R L - \frac{11}{9}T_R \right) \right] C_i^{(n_l),1} + \\
&+ \left[\alpha_s^{(n_l+1)^2}(Q^2) - \frac{4}{3}T_R L \alpha_s^{(n_l+1)^3}(Q^2) \right] C_i^{(n_l),2} + \alpha_s^{(n_l+1)^3}(Q^2) C_i^{(n_l),3} = \\
&= C_i^{(n_l),0} + \alpha_s^{(n_l+1)}(Q^2) C_i^{(n_l),1} + \alpha_s^{(n_l+1)^2}(Q^2) \left[- \frac{2}{3}T_R L C_i^{(n_l),1} + C_i^{(n_l),2} \right] + \\
&+ \alpha_s^{(n_l+1)^3}(Q^2) \left[- \left(- \frac{4}{9}T_R^2 L^2 + \frac{11}{3}T_R L - \frac{11}{9}T_R \right) C_i^{(n_l),1} + \right. \\
&\left. - \frac{4}{3}T_R L C_i^{(n_l),2} + C_i^{(n_l),3} \right]
\end{aligned} \tag{5.23}$$

where we explicitly separated the contributions to the massive coefficient functions $C_i^{(n_l)}$ in terms of the coupling $\alpha_s^{(n_l+1)}$.

Equations (5.14) and (5.15) must be rewritten with all the PDFs and the coupling evaluated at Q^2. Starting from the PDFs of the light quarks and noting that the lowest order of α_s in (5.15) is two, it is sufficient a

development of the Altarelli-Parisi equations up to the first order:

$$\begin{aligned} f_q^{(n_l+1)}(x,Q^2) &= f_q^{(n_l+1)}(x,m_h^2) + \alpha_s^{(n_l+1)}(m_h^2) L \sum_j P_{qj}^{(n_l+1),0} \otimes f_j^{(n_l+1)}(m_h^2) \simeq \\ &\simeq f_q^{(n_l+1)}(x,m_h^2) + \alpha_s^{(n_l+1)}(m_h^2) L \sum_j P_{qj}^{(n_l+1),0} \otimes f_j^{(n_l+1)}(Q^2) \\ \rightarrow f_q^{(n_l+1)}(x,m_h^2) &= f_q^{(n_l+1)}(x,Q^2) - \alpha_s^{(n_l+1)}(m_h^2) L \sum_j P_{qj}^{(n_l+1),0} \otimes f_j^{(n_l+1)}(Q^2) \end{aligned} \tag{5.24}$$

The same strategy is used for the coupling. More precisely, in (5.15) all the α_s are in the n_l scheme and at the scale m_h^2. The lowest power of the coupling in this same equation is two: considering that

$$\alpha_s^{(n_l)}(m_h^2) = \alpha_s^{(n_l+1)}(m_h^2) + \mathcal{O}(\alpha_s^3),$$

up to α_s^3 all the $\alpha_s^{(n_l)}$ can be substituted with $\alpha_s^{(n_l+1)}$. Evolving up to Q^2 one obtains:

$$\begin{aligned} \alpha_s^{(n_l+1)}(Q^2) &= \alpha_s^{(n_l+1)}(m_h^2) - \beta_0^{(n_l+1)} L {\alpha_s^{(n_l+1)}}^2(m_h^2) \simeq \\ &\simeq \alpha_s^{(n_l+1)}(m_h^2) - \beta_0^{(n_l+1)} L {\alpha_s^{(n_l+1)}}^2(Q^2) \\ \rightarrow \alpha_s^{(n_l+1)}(m_h^2) &= \alpha_s^{(n_l+1)}(Q^2) + \beta_0^{(n_l+1)} L {\alpha_s^{(n_l+1)}}^2(Q^2) \end{aligned} \tag{5.25}$$

The following substitutions are thus straightforward:

- ${\alpha_s^{(n_l+1)}}^2(m_h^2) \longrightarrow {\alpha_s^{(n_l+1)}}^2(Q^2) + 2\beta_0^{(n_l+1)} L {\alpha_s^{(n_l+1)}}^3(Q^2)$
- ${\alpha_s^{(n_l+1)}}^3(m_h^2) \longrightarrow {\alpha_s^{(n_l+1)}}^3(Q^2)$

With the previous considerations, equation (5.15) with all the PDFs and

the coupling evaluated in Q^2 becomes:

$$
\begin{aligned}
&f_q^{(n_l)}(Q^2) = f_q^{(n_l+1)}(Q^2) - {\alpha_s^{(n_l+1)}}^2 \sum_j K_{qj} \otimes f_j^{(n_l+1)} + \\
&- 2\beta_0^{(n_l+1)} L {\alpha_s^{(n_l+1)}}^3 \sum_j K_{qj} \otimes f_j^{(n_l+1)} + {\alpha_s^{(n_l+1)}}^3 L \sum_j \left(K \otimes P^{(n_l+1),0} \right)_{qj} \otimes f_j^{(n_l+1)} + \\
&- {\alpha_s^{(n_l+1)}}^2 \frac{2T_R}{3} \frac{L^2}{2} \sum_{j=q,\bar{q}} P_{qj}^{(n_l),0} \otimes f_j^{(n_l+1)} + \\
&- 2\beta_0^{(n_l+1)} L {\alpha_s^{(n_l+1)}}^3 \frac{2T_R}{3} \frac{L^2}{2} \sum_{j=q,\bar{q}} P_{qj}^{(n_l),0} \otimes f_j^{(n_l+1)} + \\
&+ {\alpha_s^{(n_l+1)}}^3 \frac{2T_R}{3} \frac{L^3}{2} \sum_{j=q,\bar{q}} P_{qj}^{(n_l),0} \otimes P_{jk}^{(n_l+1),0} \otimes f_k^{(n_l+1)} + \\
&- {\alpha_s^{(n_l+1)}}^2 L(-\Delta_{qq}) \otimes f_q^{(n_l+1)} - 2\beta_0^{(n_l+1)} L^2 {\alpha_s^{(n_l+1)}}^3 (-\Delta_{qq}) \otimes f_q^{(n_l+1)} + \\
&+ {\alpha_s^{(n_l+1)}}^3 L^2 \sum_j (-\Delta_{qq}) \otimes P_{qj}^{(n_l+1),0} \otimes f_j^{(n_l+1)} - \alpha_s^3 \sum_j K_{qj}^1 \otimes f_j^{(n_l+1)} + \\
&- {\alpha_s^{(n_l+1)}}^3 \frac{L^3}{6} \sum_j \left[(P^0 \otimes P^0 \otimes P^0)^{(n_l+1)})_{qj} - (P^0 \otimes P^0 \otimes P^0)^{(n_l)})_{qj} \right] \otimes f_j^{(n_l+1)} + \\
&+ \frac{11}{9} T_R {\alpha_s^{(n_l+1)}}^3 L \sum_j P_{qj}^{(n_l),0} \otimes f_j^{(n_l+1)} + \frac{L^2}{2} \frac{19}{3} T_R {\alpha_s^{(n_l+1)}}^3 \sum_j P_{qj}^{(n_l),0} \otimes f_j^{(n_l+1)} + \\
&+ \frac{L^3}{2} {\alpha_s^{(n_l+1)}}^3 \sum_j \left[\beta_0^{(n_l+1)} (P^0 \otimes P^0)_{qj}^{(n_l+1)} - \beta_0^{(n_l)} (P^0 \otimes P^0)_{qj}^{(n_l)}) \otimes f_j^{(n_l+1)} \right] + \\
&- \frac{L^3}{3} {\alpha_s^{(n_l+1)}}^3 \left(\frac{2}{3} T_R\right)^2 \sum_j P_{qj}^{(n_l),0} \otimes f_j^{(n_l+1)} + \frac{L^3}{3} {\alpha_s^{(n_l+1)}}^3 \beta_0^{(n_l)} (\frac{4}{3} T_R) \sum_j P_{qj}^{(n_l),0} \otimes f_j^{(n_l+1)} + \\
&+ \beta_0^{n_l} {\alpha_s^{(n_l+1)}}^3 L^2 (-\Delta_{qq}) \otimes f_q^{(n_l+1)} - {\alpha_s^{(n_l+1)}}^3 \frac{2}{3} T_R L^2 \sum_j P_{qj}^{(n_l+1),1} \otimes f_j^{(n_l+1)} - \\
&- {\alpha_s^{(n_l+1)}}^3 L^2 \sum_j \left[(P^0 \otimes P^1)_{qj}^{(n_l+1)} - (P^0 \otimes P^1)_{qj}^{(n_l)} \right] \otimes f_j^{(n_l+1)} + \\
&- {\alpha_s^{(n_l+1)}}^3 L \sum_j \left[P^{(n_l+1),2} - P^{(n_l),2} \right]_{qj} \otimes f_j^{(n_l+1)} - {\alpha_s^{(n_l+1)}}^3 L \sum_j \left(P^{(n_l),0} \otimes K \right)_{qj} \otimes f_j^{(n_l+1)}
\end{aligned}
\tag{5.26}
$$

This same calculations can be performed also in the gluon sector. The gluon coefficient functions start at $\mathcal{O}(\alpha_s)$, so a development of the gluon PDF

up to the second order is sufficient.

$$
\begin{aligned}
&f_g^{(n_l)}(Q^2) = f_g^{(n_l+1)}(Q^2) + \alpha_s^{(n_l+1)} L \frac{2T_R}{3} f_g^{(n_l+1)} + \\
&+ \alpha_s^{(n_l+1)^2} \beta_0^{(n_l+1)} L^2 \frac{2T_R}{3} f_g^{(n_l+1)} - \alpha_s^{(n_l+1)^2} L^2 \frac{2T_R}{3} \sum_j P_{gj}^{(n_l+1),0} \otimes f_j^{(n_l)} + \\
&- \alpha_s^{(n_l+1)^2} \sum_j K_{gj} \otimes f_j^{(n_l+1)} + \frac{2T_R}{3} \alpha_s^{(n_l+1)^2} \frac{L^2}{2} P_{gg}^{(n_l),0} \otimes f_g^{(n_l+1)} + \\
&+ \alpha_s^{(n_l+1)^2} \frac{L^2}{2} \beta_0^{(n_l)} \left(- \frac{2T_R}{3} \right) f_g^{(n_l+1)} + \\
&- \alpha_s^{(n_l+1)^2} L \sum_j \left[P_{gj}^{(n_l+1),1} - P_{gj}^{(n_l),1} \right] \otimes f_j^{(n_l+1)}
\end{aligned}
\tag{5.27}
$$

We have now all the ingredients that are required for the evaluation of B_i defined in (5.19) at order α_s^3.

Firstly, we can consider the light contribution to the structure function. The basic idea is substituting (5.23), (5.26) and (5.27) into equation (5.18) and obtaining the coefficient $B_{i,l}$ making a comparison with equation (5.19).

With these substitutions one can find:

$$
\begin{aligned}
B^3_{q,l} = C^{(n_l),0}_{q,l} \otimes \Bigg[& - 2\beta_0^{(n_l+1)} L K_{qq} + L\Big(K \otimes P^{(n_l+1),0}\Big)_{qq} - 2\beta_0^{(n_l+1)} L \frac{2T_R}{3}\frac{L^2}{2} P^{(n_l),0}_{qq} + \\
& + \frac{2T_R}{3}\frac{L^3}{2} P^{(n_l),0}_{qq} \otimes P^{(n_l+1),0}_{qq} - 2\beta_0^{(n_l+1)} L^2(-\Delta_{qq}) + L^2(-\Delta_{qq}) \otimes P^{(n_l+1),0}_{qq} - K^1_{qq} + \\
& + \frac{11}{9} T_R L P^{(n_l),0}_{qq} - \frac{L^3}{6}\big[\big(P^0 \otimes P^0 \otimes P^0\big)^{(n_l+1)}_{qq} - \big(P^0 \otimes P^0 \otimes P^0\big)^{(n_l)}_{qq}\big] + \\
& + \frac{L^2}{2}\frac{19}{3} T_R P^{(n_l),0}_{qq} + \frac{1}{2} L^3 [\beta_0^{(n_l+1)} (P^0 \otimes P^0)^{(n_l+1)}_{qq} - \beta_0^{(n_l)} (P^0 \otimes P^0)^{(n_l)}_{qq}] + \\
& - \frac{1}{3} L^3 \left(\frac{2T_R}{3}\right)^2 P^{(n_l),0}_{qq} + \frac{L^3}{3}\beta_0^{(n_l)} \frac{4T_R}{3} P^{(n_l),0}_{qq} + \beta_0^{(n_l)} L^2(-\Delta_{qq}) - \frac{2T_R}{3} L^2 P^{(n_l+1),1}_{qq} + \\
& - L^2 [(P^0 \otimes P^1)^{(n_l+1)}_{qq} - (P^0 \otimes P^1)^{(n_l)}_{qq}] - L[P^{(n_l+1),2}_{qq} - P^{(n_l),2}_{qq}] - L\Big(P^{(n_l),0} \otimes K\Big)_{qq}\Bigg] + \\
& + C^{(n_l),1}_{q,l} \otimes \Bigg[- K_{qq} - \frac{2T_R}{3}\frac{L^2}{2} P^{(n_l),0}_{qq} - L(-\Delta_{qq})\Bigg] + \\
& + \Bigg[- (-\frac{4}{9} {T_R}^2 L^2 + \frac{11}{3} T_R L - \frac{11}{9} T_R) C^{(n_l),1}_{q,l} - \frac{4}{3} T_R L C^{(n_l),2}_{q,l} + C^{(n_l),3}_{q,l}\Bigg] + \\
& + C^{(n_l),1}_{g,l} \otimes \Bigg[- L^2 \frac{2T_R}{3} P^{(n_l+1),0}_{gq} - K_{gq} - L[P^{(n_l+1),1}_{gq} - P^{(n_l),1}_{gq}]\Bigg] + \\
& + C^{(n_l),0}_{\bar{q},l} \Bigg[L\Big(K \otimes P^{(n_l+1),0}\Big)_{\bar{q}q} - K^1_{\bar{q}q} - \frac{L^3}{6}[(P^0 \otimes P^0 \otimes P^0)^{(n_l+1),0}_{\bar{q}q} - (P^0 \otimes P^0 \otimes P^0)^{(n_l),0}_{\bar{q}q}] + \\
& + \frac{1}{2} L^3 [\beta_0^{(n_l+1)} (P^0 \otimes P^0)^{(n_l+1)}_{\bar{q}q} - \beta_0^{(n_l)} (P^0 \otimes P^0)^{(n_l)}_{\bar{q}q}] - \frac{2T_R}{3} L^2 P^{(n_l+1),1}_{\bar{q}q} + \\
& - L^2 ((P^0 \otimes P^1)^{(n_l+1)}_{\bar{q}q} - (P^0 \otimes P^1)^{(n_l)}_{\bar{q}q}) - L(P^{(n_l+1),2}_{\bar{q}q} - P^{(n_l),2}_{\bar{q}q}) - L\Big(P^{(n_l),0} \otimes K\Big)_{\bar{q}q}\Bigg]
\end{aligned}
\tag{5.28}
$$

where the first three square brackets come from the quark PDFs, the fourth square bracket is linked to the gluon PDF and the last lines are the antiquark contribution. The $B_{i,l}$ coefficients for the antiquarks $B_{\bar{q},l}$ can be obtained with the substitution $q \to \bar{q}$ in the above equation.

The same calculations can be done for the gluon coefficient function:

$$
\begin{aligned}
B^3_{g,l} = {} & C^{(n_l),1}_{g,l} \otimes \Bigg[\beta_0^{(n_l+1)} L^2 \frac{2}{3} T_R - L^2 \frac{2}{3} T_R P_{gg}^{(n_l+1),0} - K_{gg} + \frac{2}{3} T_R \frac{L^2}{2} P_{gg}^{(n_l),0} + \\
& + \frac{L^2}{2} \beta_0^{(n_l)} (-\frac{2}{3} T_R) - L(P_{gg}^{(n_l+1),1} - P_{gg}^{(n_l),1}) \Bigg] + \Bigg[- \frac{2}{3} T_R C_{g,l}^{(n_l),1} + C_{g,l}^{(n_l),2} \Bigg] (L \frac{2}{3} T_R) + \\
& + \Bigg[- (-\frac{4}{9} {T_R}^2 L^2 + \frac{11}{3} T_R L - \frac{11}{9} T_R) C_{g,l}^{(n_l),1} - \frac{4}{3} T_R L C_{g,l}^{(n_l),2} + C_{g,l}^{(n_l),3} \Bigg] + \\
& + C_{q,l}^{(n_l),0} \otimes \Bigg[- 2\beta_0^{(n_l+1)} L K_{qg} + L \Bigg(K \otimes P^{(n_l+1),0} \Bigg)_{qg} + \frac{2T_R}{3} \frac{L^3}{2} P_{qq}^{(n_l),0} \otimes P_{qg}^{(n_l+1),0} + \\
& + L^2 (-\Delta_{qq}) \otimes P_{qg}^{(n_l+1),0} - K_{qg}^1 + \frac{11}{9} T_R L P_{qg}^{(n_l),0} + \\
& - \frac{L^3}{6} [(P^0 \otimes P^0 \otimes P^0)_{qg}^{(n_l+1),0} - (P^0 \otimes P^0 \otimes P^0)_{qg}^{(n_l),0}] + \frac{L^2}{2} \frac{19}{3} T_R P_{qg}^{(n_l),0} + \\
& + \frac{L^3}{2} [\beta_0^{(n_l+1)} (P^0 \otimes P^0)_{qg}^{(n_l+1)} - \beta_0^{(n_l)} (P^0 \otimes P^0)_{qg}^{(n_l)}] - \frac{L^3}{3} (\frac{2T_R}{3})^2 P_{qg}^{(n_l),0} + \\
& + \frac{L^3}{3} \beta_0^{(n_l)} (\frac{4T_R}{3}) P_{qg}^{(n_l),0} - \frac{2T_R}{3} L^2 P_{qg}^{(n_l+1),1} - L^2 [(P^0 \otimes P^1)_{qg}^{(n_1+1)} - (P^0 \otimes P^1)_{qg}^{(n_1)})] + \\
& - L(P^{(n_l+1),2} - P^{(n_l),2})_{qg} - L \Bigg(P^{(n_l)} \otimes K \Bigg)_{qg} \Bigg] + \\
& C_{g,l}^{(n_l),1} \otimes \Bigg[- K_{qg} \Bigg] + \Bigg[q \to \bar{q} \Bigg]
\end{aligned}
\tag{5.29}
$$

The first three lines come from the gluon PDF while the other terms are linked to quarks and antiquarks contribution. The antiquarks contribution can be obtained simply with the substitution $q \to \bar{q}$ and it has thus been included in a compact form in the last bracket.

Using equations (5.28) and (5.29), we can recover the massive structure function with the PDFs and the coupling expressed in the massless scheme. The third order contribution reads:

$$
F_l^{(n_l),3} = x \sum_{i=q,\bar{q},g} \int_x^1 \frac{dy}{y} B^3_{i,l} \left(\frac{x}{y}, \frac{Q^2}{m_h^2} \right) f_i^{(n_l+1)}(y, Q^2) \tag{5.30}
$$

where the coefficients $B_{i,l}$ are defined in (5.28) and (5.29).

The FONLL light structure function is constructed as the sum of the massive structure function and the difference term introduced in (4.17):

$$
F_l^{FONLL,3}(x, Q^2) = F_l^{(n_l),3}(x, Q^2) + F_l^{(d),3}(x, Q^2) \tag{5.31}
$$

The difference term can be obtained as follows:

$$\begin{aligned} F_l^{(d),3} &= F_l^{(n_l+1),3} - F_l^{(n_l,0),3} = \\ &= x\int_x^1 \frac{dy}{y} \sum_{i=q,\bar{q},g,h,\bar{h}} C_{i,l}^{(n_l+1),3} f_i^{(n_l+1)} - x\int_x^1 \frac{dy}{y} \sum_{i=q,\bar{q},g} B_{i,l}^{(n_l,0),3} f_i^{(n_l+1)} = \\ &= x\int_x^1 \frac{dy}{y} \sum_{i=q,\bar{q},g} \left[C_{i,l}^{(n_l+1),3} - B_{i,l}^{(0),3} \right] f_i^{(n_l+1)} + x\int_x^1 \frac{dy}{y} \sum_{i=h,\bar{h}} C_{i,l}^{(n_l+1),3} f_i^{(n_l+1)} \end{aligned} \tag{5.32}$$

where the coefficients $B_{i,l}^{(0),3}$ terms are the massless limits of the $B_{i,l}^3$ previously defined. The light FONLL structure function is now complete.

Using the same strategy, one can obtain the FONLL heavy structure function. First of all, it is necessary to calculate the coefficients $B_{i,h}$ through which express the massive structure function in terms of the massless PDFs and coupling. The heavy coefficient functions $C_{i,h}$ for i corresponding to any light quark start at α_s^2 while the gluon coefficient $C_{g,h}$ starts contributing at α_s.

$$\begin{aligned} B_{q,h}^3 =& \left[-\frac{4}{3} T_R L C_{q,h}^{(n_l),2} + C_{q,h}^{(n_l),3} \right] + \\ &+ C_{g,h}^{(n_l),1} \otimes \left[-L^2 \frac{2T_R}{3} P_{qq}^{(n_l+1),0} - K_{gq} - L(P_{gq}^{(n_l+1),1} - P_{gq}^{(n_l),1}) \right] \end{aligned} \tag{5.33}$$

$$\begin{aligned} B_{g,h}^3 =& C_{g,h}^{(n_l),1} \otimes \left[\beta_0^{(n_l+1)} L^2 \frac{2}{3} T_R - L^2 \frac{2}{3} T_R P_{gg}^{(n_l+1),0} - K_{gg} + \right. \\ &\left. + \frac{2}{3} T_R \frac{L^2}{2} P_{gg}^{(n_l),0} + \frac{L^2}{2} \beta_0^{(n_l)} (-\frac{2}{3} T_R) - L(P_{gg}^{(n_l+1),1} - P_{gg}^{(n_l),1}) \right] + \\ &+ \left[-\frac{2}{3} T_R C_{g,h}^{(n_l),1} + C_{g,h}^{(n_l),2} \right] (L\frac{2}{3} T_R) + \\ &+ \left[-(-\frac{4}{9} {T_R}^2 L^2 + \frac{11}{3} T_R L - \frac{11}{9} T_R) C_{g,h}^{(n_l),1} - \frac{4}{3} T_R L C_{g,h}^{(n_l),2} + C_{g,h}^{(n_l),3} \right] \end{aligned} \tag{5.34}$$

The third order contribution of the massive structure function is thus:

$$F_h^{(n_l),3} = x \sum_{i=q,\bar{q},g} \int_x^1 \frac{dy}{y} B_{i,h}^3 \left(\frac{x}{y}, \frac{Q^2}{m_h^2} \right) f_i^{(n_l+1)}(y, Q^2) \tag{5.35}$$

with $B_{i,h}$ defined in (5.33) and (5.34). The heavy difference term is:

$$\begin{aligned} F_h^{(d),3} &= F_h^{(n_l+1),3} - F_h^{(n_l,0),3} = \\ =&x\int_x^1 \frac{dy}{y} \sum_{i=q,\bar{q},g,h,\bar{h}} C_{i,h}^{(n_l+1),3} f_i^{(n_l+1)} - x\int_x^1 \frac{dy}{y} \sum_{i=q,\bar{q},g} B_{i,h}^{(n_l,0),3} f_i^{(n_l+1)} = \\ =&x\int_x^1 \frac{dy}{y} \sum_{i=q,\bar{q},g} \left[C_{i,h}^{(n_l+1),3} - B_{i,h}^{(0),3}\right] f_i^{(n_l+1)} + x\int_x^1 \frac{dy}{y} \sum_{i=h,\bar{h}} C_{i,h}^{(n_l+1),3} f_i^{(n_l+1)} \end{aligned} \tag{5.36}$$

Here $C_{i,h}^{(n_l+1),3}$ are the massless scheme $\mathcal{O}(\alpha_s^3)$ contributions to the standard coefficient functions for the production of a quark of electric charge e_h with the heavy quark treated as a massless flavour; $B_{i,h}^{(0),3}$ are the massless limits of (5.33) and (5.34). The $\mathcal{O}(\alpha_s^3)$ contribution to the FONLL heavy structure function is now complete:

$$F_h^{FONLL,3}(x,Q^2) = F_h^{(n_l),3}(x,Q^2) + F_h^{(d),3}(x,Q^2) \tag{5.37}$$

The implementation of the FONLL electromagnetic structure functions up to α_s^3 is now fully defined.

With the actual knowledge of massive coefficient functions, it is impossible to numerically study the structure functions we explicitly obtained in this section. In fact, many of the massive coefficient functions that are required for the calculation are not analytically known (in most cases, they are known only in the asymptotic region. For updated reviews, see [11, 12, 13]). Probably, a complete N^{3}LO matching will be performed in the next few years.

In the next section, we will analyse the matching condition for the heavy quark in detail, considering the explicit case of the charm. Even if all the terms required by the matching are not fully known, it is possible to provide a first partial result with the main goal of understanding how a α_s^3 matching can modify the perturbative charm PDF with respect to a fitted charm.

5.3 Charm PDF

In this section we analyse the matching condition for the charm PDF in the absence of an intrinsic contribution:

$$f_h^{(n_l+1)}(x,m_h^2) = f_{\bar{h}}^{(n_l+1)}(x,m_h^2) = \alpha_s^2 \int \frac{dz}{z} \sum_{j=q,\bar{q},g} K_{hj}(z) f_j^{(n_l)}(\frac{x}{z},m_h^2) + \\ + \alpha_s^3 \int \frac{dz}{z} \sum_{j=q,\bar{q},g} K_{hj}^1(z) f_j^{(n_l)}(\frac{x}{z},m_h^2) + \mathcal{O}(\alpha_s^4) \tag{5.38}$$

This equation can be rewritten in terms of the (n_l+1) PDFs only without any modification thanks to the matching condition of the light quarks and the gluon described in the previous section: at a scale equal to the heavy quark mass, they satisfy a matching condition of the form $f_i^{(n_l)}(x,m_h^2) = f_i^{(n_l+1)}(x,m_h^2) + \mathcal{O}(\alpha_s^2)$, in which the term that is linear in α_s is zero. Clearly, if we consider the charm PDF at a different scale numerous terms arise due to the DGLAP evolution equation.

The coefficients K_{ij} are commonly used for the determination of the charm PDF up to α_s^2: in fact, at this order they are analytically known [4]. Recently, the K_{ij}^1 terms have been partially obtained [11, 12]: in this thesis we perform a matching for the charm PDF one order higher than what has been usually performed till now. Even if our result does not provide the correct numerical result, all the leading terms of K_{ij}^1 have been calculated and they are sufficient for a first phenomenological analysis.

From now on, we will refer to these terms using the same notation of the cited papers, which means A_{Qq} and A_{Qg}. The incomplete term is A_{Qg}, while A_{Qq} is analytically known.

The calculation has been performed at a scale equal to the pole mass of the charm, $M = 1.51\text{GeV}$. The choice of the scale is determined by the fact that A_{Qq} and A_{Qg} are expressed in terms of the pole mass of the heavy quark, so that all the terms proportional to $\log(Q^2/M^2)$ are set equal to zero.

This chapter is structured as follows: in the first section we discuss the calculation of the matching terms A_{Qq} and A_{Qg} as described in the cited papers. We then provide a discussion on their analytic forms and the problems related to a direct use of them. The second section is dedicated to our numerical implementation. The last part is a discussion of our result.

5.3.1 Analytic calculation

The OMEs A_{ij} obeys the expansion

$$A_{ij}\left(\frac{m_h^2}{\mu^2}\right) = \langle j|O_i|j\rangle = \delta_{ij} + \sum_{l=1}^{\infty} \alpha_s^l A_{ij}^{(l)} \tag{5.39}$$

of the twist-2 quark operators O_i between partonic states $|i\rangle$. The two matching terms A_{Qq} and A_{Qg} have been (partially) calculated at α_s^3 in [11, 12] and have been directly obtained for our implementation from the authors.

These OMEs are obtained generating all the Feynman diagrams which contribute to the different channels (production of an heavy quark starting from light quarks and gluons at α_s^3), adding the corresponding operator insertion as effective vertices of the theory. These graphs are obtained using a fortran-based program QGRAPH [50].

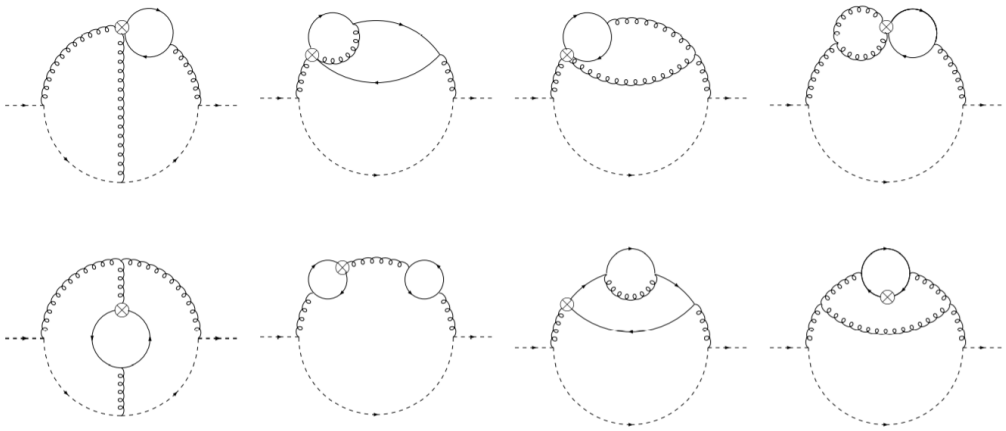

Figure 5.2: Sample of diagrams contributing to $A_{Qq}^{(3)}$. The dashed arrow lines represent massless quarks, while the solid arrow lines represent massive quarks. Curly lines are gluons. The symbol $\otimes$ denotes the local operator insertion.

In our case, 125 diagrams contribute to A_{Qq} and 1358 contribute to A_{Qg}. A sample of this contributions at α_s^3 is given in 5.2.

Calculations are then reduced to master integrals using integration by parts IBP relations [27], which is one of the most widely used methods in multi-loop calculations as it reduces a complicated Feynman diagram in terms of a limited number of integrals. Nowadays, this reduction is automated

thanks to different algorithms. [51]. Depending on their complexity, different calculation methods exist to compute these integrals. The simplest integrals can be expressed in terms of (generalized) hypergeometric functions, otherwise one can construct a Mellin-Barnes representation [31], which expresses a massive propagator in terms of a contour integral involving a massless one. For more complicated integrals, one usually adopts the differential equation method [32], which expresses Feynman integrals in terms of canonical differential equations through specific algorithms that have led to a certain degree of automation in calculations at NNLO involving many particles.

The term A_{Qq} is analytically known while A_{Qg} presents some missing terms. We expect that our calculation is not so far from the complete one because the most significant part of A_{Qg} is analytically known (1122 Feynman diagrams over a total of 1358). Furthermore, missing terms are subleading in the colour factors, as they do not present the highest powers possible (whose terms are included in our calculation).

The two OMEs are obtained in analytic form N-space. Explicit expressions can be found in [11, 12, 13]. They present terms which explicitly depend on the number of flavours n_f.

They are expressed in terms of harmonic sums [46], defined as

$$S_{b,\vec{a}}(N) = \sum_{k=1}^{N} \frac{(sgn(b))^k}{k^{|b|}} S_{\vec{a}}(k), \quad S_\emptyset = 1, \quad b, a_i \in \mathbb{Z} \setminus \{0\} \tag{5.40}$$

and generalized harmonic sums [12] (the 3-loop matching is the first case in which these terms appear):

$$S_{b,\vec{a}}(c,\vec{d})(N) = \sum_{k=1}^{N} \frac{c^k}{k^b} S_{\vec{a}}(\vec{d})(k), \quad S_\emptyset = 1, \quad b, a_i \in \mathbb{N} \setminus \{0\}, \quad c, d_i \in \mathbb{Z} \setminus \{0\} \tag{5.41}$$

In particular, in A_{Qq} and A_{Qg} there are (generalized) harmonic sums up to *depth* five. The depth represents the number of components of the vector $\vec{a}$ plus one (it is the effective number of indexes of the harmonic sum $S_{b,\vec{a}}$).

At this point it is possible to evaluate the two OMEs A_{Qq} and A_{Qg}, making a first comparison between their values up to α_s^2 and α_s^3. This evaluation has been done using the Mathematica package *Harmonic Sums* [33], which is a package that deals with special functions (harmonic sums, S-sums, cyclotomic sums, harmonic polylogarithms,..) in an algorithmic fashion.

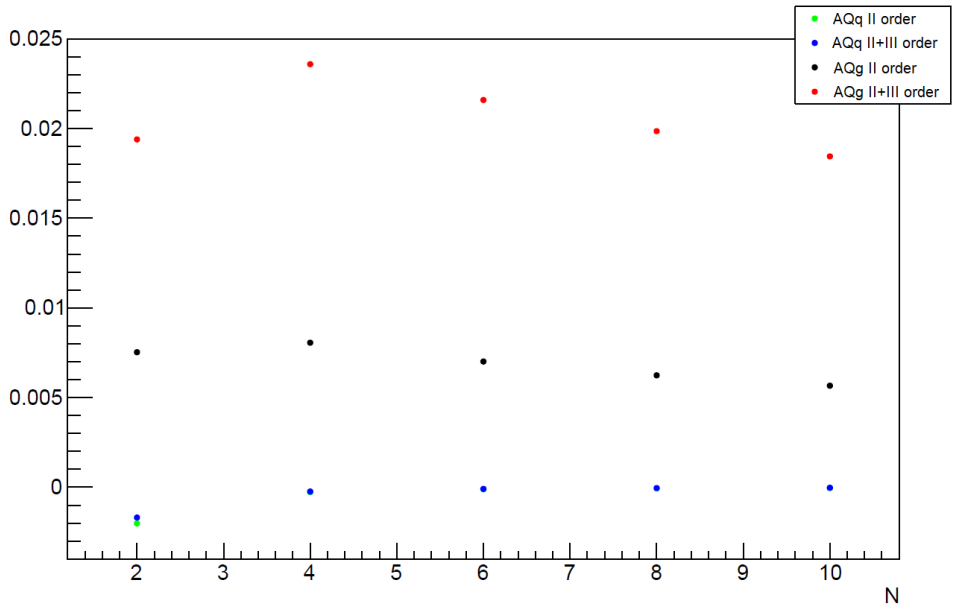

Figure 5.3: OMEs at α_s^2 and α_s^3 in N-space at 1.51 GeV. N is even because of the correct analytic continuation concerning the singlet term Σ, which is defined as sum of all quark and antiquark PDFs.

A first interesting feature that can be derived from 5.3 is that the α_s^3 contribution in A_{Qg} is particularly higher than the α_s^2 part: more precisely, α_s^3 momenta are almost three times grater than the α_s^2 ones. For this reason, we expect an important increase in the gluon contribution in the matching of the charm PDF. By contrast, the terms related to quarks A_{Qq} are almost identical in the two cases.

5.3.2 Numerical implementation

The matching condition for the charm PDF can be computed in two different ways: on the one hand, calculations can be performed in N space and then one can implement a numerical inverse Mellin transform in order to obtain a result in x-space. On the other hand, calculations can be performed directly in x-space, which requires the explicit expressions for the OMEs in terms of x.

As for the first option, the inverse Mellin transform is defined as

$$f(x) = \frac{1}{2\pi i} \int_{c-i\infty}^{c+i\infty} dN x^{-N} \widetilde{f}(N) \tag{5.42}$$

where $c \in \mathfrak{R}$ is chosen in order to make the integral converge. In general, a numerical inverse Mellin transform is performed on a path tilted with an acute angle with respect to the negative real axis starting from a real point which lies at the right of the last singularity. On this path, the integral converges fast.

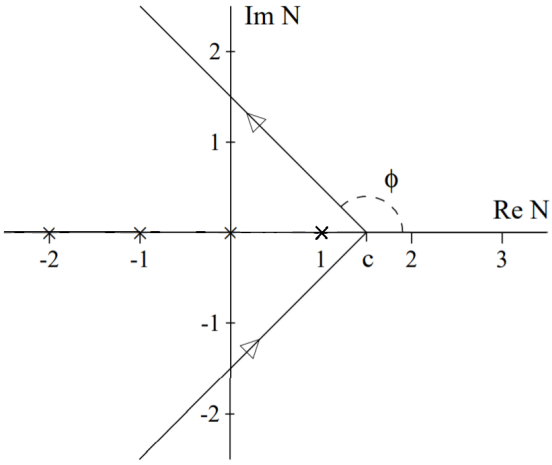

Figure 5.4: Complex path commonly used to perform a numerical inverse Mellin transform.

This calculation requires the knowledge of the OMEs on the whole complex plane. However, using the recursion relations (5.40) and (5.41), the harmonic sums can be evaluated only for integer values of N.

There are many examples of harmonic sums whose analytic continuations are now well-known and have been deeply studied, such as the easiest harmonic sum $S_1(N)$. This function can be analytically continued as a polygamma function through the relation:

$$S_1(N) = \psi(N) + \gamma_E \tag{5.43}$$

The polygamma function $\psi(N)$ is defined starting from the Γ function

$$\psi(N) = \frac{\Gamma'(N)}{\Gamma(N)} \tag{5.44}$$

and γ_E=0.5772156 is the Euler-Mascheroni constant .

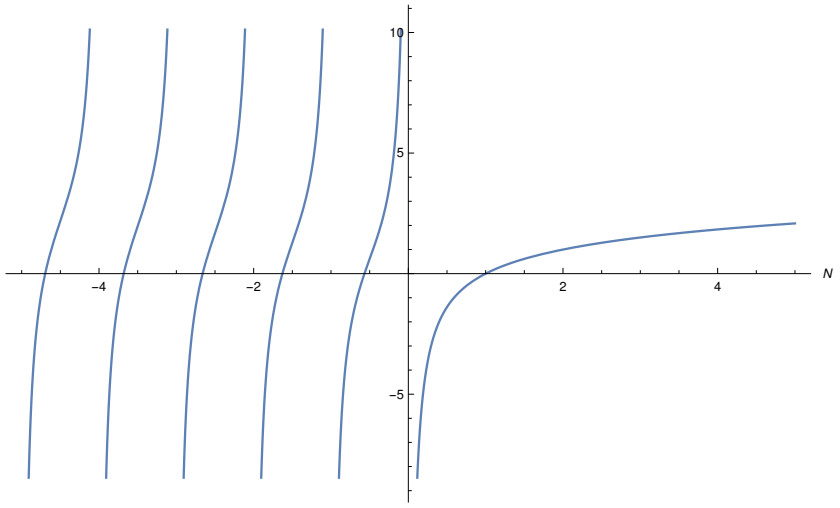

Figure 5.5: Analytic continuation in the complex plane of the harmonic sum $S_1(N)$.

More complicated harmonic sums can be expressed in terms of the easiest ones using many recursion relations (see for example appendix A in [47]). Anyway, these relations are not sufficient for calculating all the analytic continuations that appear in our OMEs: in order to overcome this problem, we decided to work directly in x-space. In fact, these harmonic sums can be expressed in integral form, which means as the Mellin transform of certain functions. These relations are implemented in the package *Harmonic Sums* that is thus been used for analytically inverting the two OMEs in x-space.

In x-space, harmonic sums become harmonic polylogarithms [34], which are defined as iterated integrals:

$$H_{b,\vec{a}} = \int_0^z f_b(y) H_{\vec{a}}(y), \quad f_b \in \mathfrak{U}, \quad H_\emptyset = 1, H_{\underbrace{0,...,0}_{k}} := \frac{1}{k!} ln^k(z) \tag{5.45}$$

where $\mathfrak{U}$, called *alphabet*, is defined, in our case, as:

$$\mathfrak{U} = \left\{ \frac{dz}{z}, \frac{dz}{1-z}, \frac{dz}{1+z} \right\} \equiv \{f_0(z), f_1(z), f_{-1}(z)\} \tag{5.46}$$

The alphabet represents the set of integration kernels appearing in a given quantity.

The numerical evaluation of these harmonic polylogarithms is done using the C++ library GiNaC [35]. GiNaC is a software developed exactly in the context of calculations of higher-order corrections to elementary particle interactions which combines symbolical and numerical approaches alike. We plotted the two OMEs at α_s^2 and α_s^3 in order to understand how the important increase in the gluon term in N-space manifests in x-space.

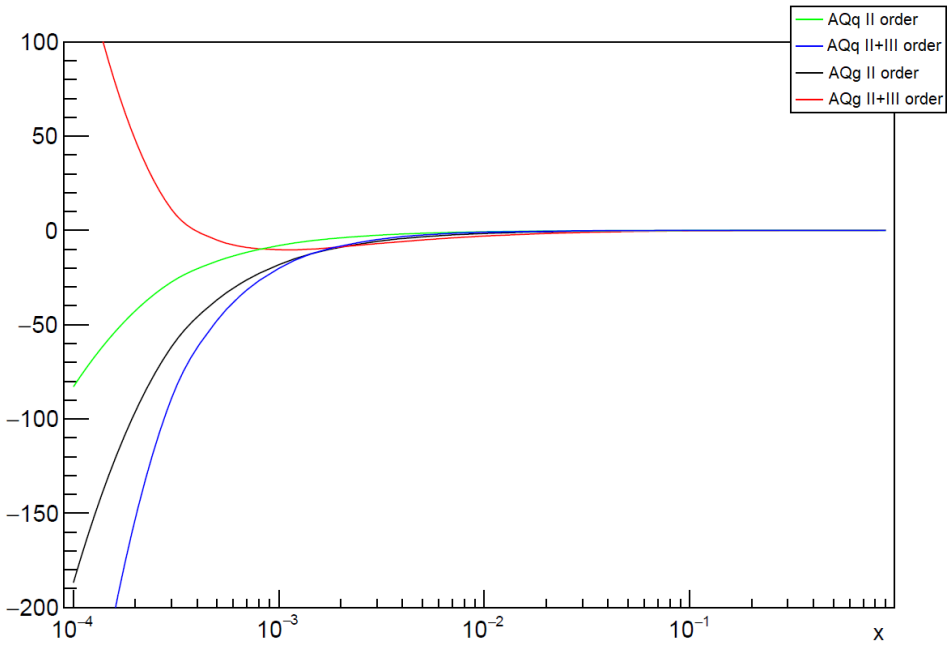

Figure 5.6: OMEs at α_s^2 and α_s^3 in x-space with a log scale at 1.51 GeV.

Our region of interest is $x \geq 10^{-3}$. We thus plotted both a log-scale and a linear-scale graph in order to highlight separately the low-x region and the high-x region. In the low-x region, the OMEs do not modify significantly when increasing the perturbative order. The main differences can be found in the very large-x region ($x > 0.6$), where A_{Qg} at α_s^3 doubles its value at α_s^2. As we noticed in N-space, A_{Qq} does not modify significantly on the whole domain. In order to verify the correctness of the calculation, we studied also x times the OMEs, which is linked to the momentum space through integration. The value obtained in N-space for N=2 must be reproduced by the integration of x times the OME, simply using the definition of the Mellin

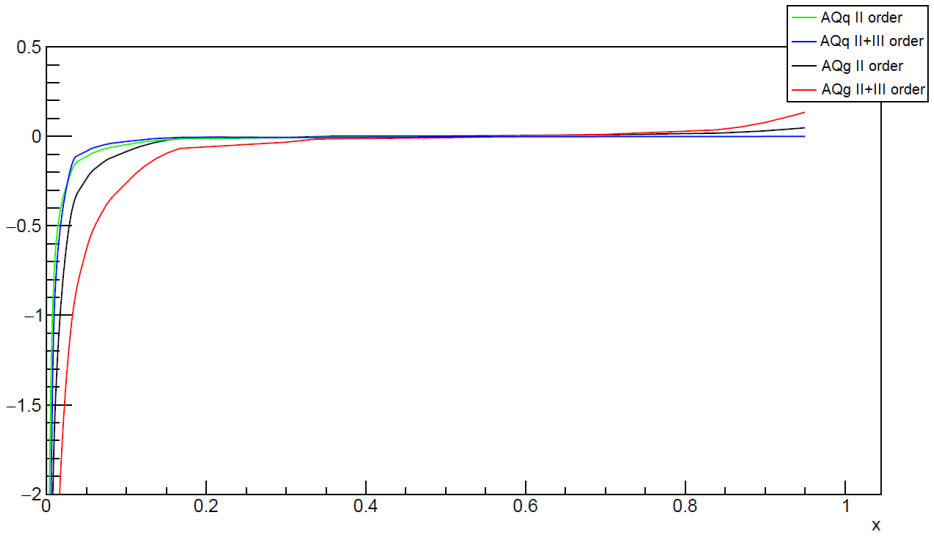

Figure 5.7: OMEs at α_s^2 and α_s^3 in x-space with a linear scale at large x at 1.51 GeV.

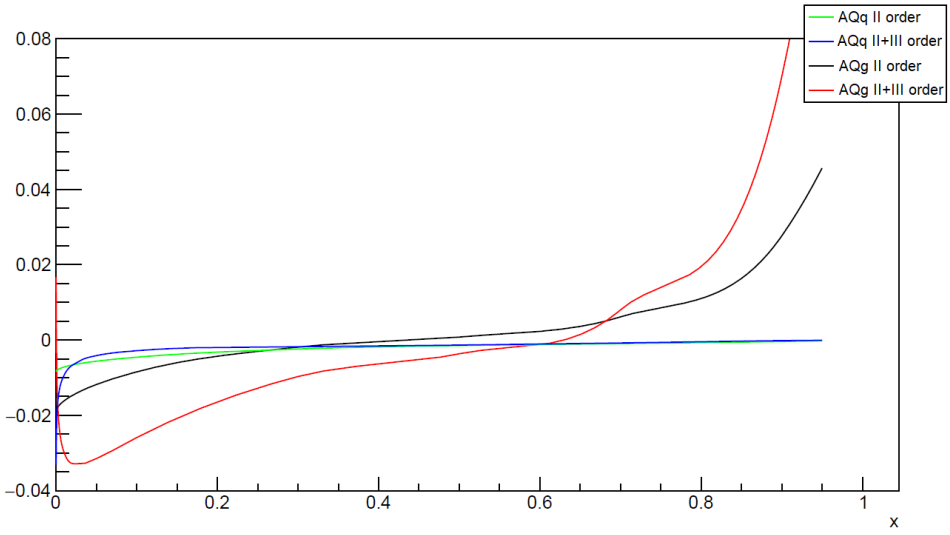

Figure 5.8: Plot of x times the OMEs with a linear scale at large x at 1.51 GeV.

transform. Again, the plot clearly shows an important contribution due to the gluon term A_{Qg}.

5.3.3 Results

We have now all the ingredients for performing the matching condition of the charm PDF. The PDFs which are required for the calculation are obtained using the the LHAPDF grids [28], through which one can evaluate PDFs starting from discretized data files. In particular, we used the PDF set NNPDF31_nnlo_as_0118 [29] from the NNPDF collaboration. The PDFs are already in x-space, so we simply need to implement the convolution between the OMEs and the PDFs. Our program is written in C++; the integration has been implemented using the gsl library [48].

The matching has been performed at 1.51 GeV.

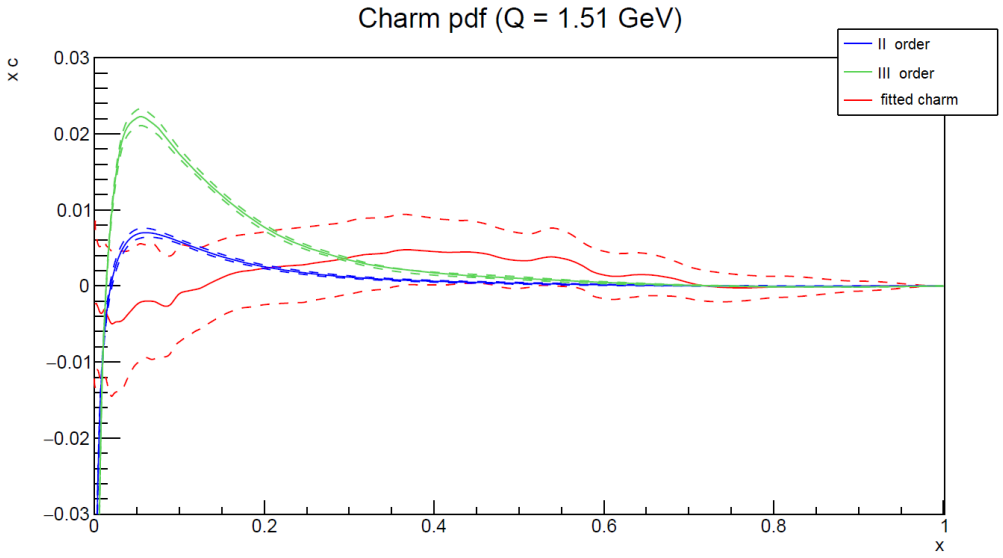

Figure 5.9: The plot shows x times the charm PDF with a linear scale comparing a fully perturbative charm up to α_s^3 and α_s^2 and a fitted charm.

In our final plots 5.9 and 5.10, we show the differences between a fully perturbative charm with a $\mathcal{O}(\alpha_s^3)$ matching, a fully perturbative charm with a $\mathcal{O}(\alpha_s^2)$ matching and a fitted charm.

- $\mathcal{O}(\alpha_s^3)$ charm PDF: the plot is obtained from (5.38) implementing a convolution between the OMEs A_{Qq} and A_{Qg} and the corresponding PDFs. The mean value is calculated using the central value of the PDF set NNPDF31_nnlo_as_0118. The main problem in this calculation is the computational time that is required: for this reason, it is impossible

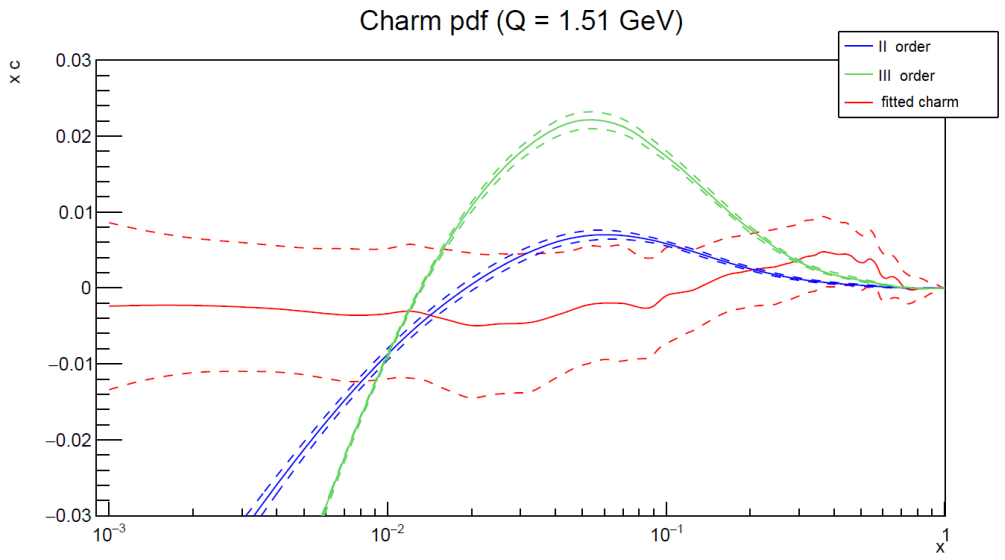

Figure 5.10: The plot shows x times the charm PDF with a log scale comparing a fully perturbative charm up to α_s^3 and α_s^2 and a fitted charm.

to obtain the error bar as the standard deviation of all the replicas, repeating the same calculation with all the PDFs provided in the set. The plotted error is obtained using the same PDF set in a so-called *hessian version*.

For hessian PDFs sets, both a central set and error sets are given. Hessian sets provide a hessian matrix of the χ^2 at the minimum whose eigenvalues are the parameters with their uncertainties $a_i \pm \sigma_{a_i}$: each error set corresponds to moving by one sigma in the positive or negative direction of each independent orthonormal Hessian eigenvector. In other words, hessian sets provides a central value f_0 and N error sets f_i, $i = 1, .., N$, for a PDF. The PDF uncertainty is defined as

$$\delta f(x, Q^2) = \sqrt{\sum_{i=1}^{N} \left(f_i(x, Q^2) - f_0(x, Q^2)\right)^2} \tag{5.47}$$

which allows to construct a *maximum* and a *minimum* PDF:

$$f(x, Q^2)_{max} = f_0(x, Q^2) + \delta f(x, Q^2) \tag{5.48}$$
$$f(x, Q^2)_{min} = f_0(x, Q^2) - \delta f(x, Q^2) \tag{5.49}$$

The error bar is obtained performing the calculation with *maximum* and *minimun* gluon and quarks PDFs.

- $\mathcal{O}(\alpha_s^2)$ charm PDF: this PDF can be obtained either as described for the $\mathcal{O}(\alpha_s^3)$ charm PDF, truncating the OMEs at the correct order, or using the set NNPDF31_nnlo_pch_as_0118, where the charm is fully perturbative. We used directly this second method while the first one was a cross check for our implementation of the code up to α_s^3. The mean value is obtained using the central PDF f_0 of the set which corresponds to

$$f_0(x, Q^2) = \frac{1}{N} \sum_{i=1}^{N} f_i(x, Q^2) \tag{5.50}$$

while the error bar is given by the standard deviation:

$$\delta f(x, Q^2) = \sqrt{\frac{1}{N-1} \sum_{i=1}^{N} \left(f_i(x, Q^2) - f_0(x, Q^2)\right)^2} \tag{5.51}$$

where the index i runs over all the replicas.

- Fitted charm PDF: this PDF is obtained from the same set NNPDF31_nnlo_as_0118 in which the charm is parametrized and determined along with light quarks and gluon PDFs. From this point of view, the distinction between the perturbatively generated component and a possible intrinsic component becomes irrelevant. The charm is treated on the same footing as the other fitted PDFs using the NNPDF methodology: its PDF is parametrized with an independent neural network with 37 free parameters, without committing to any specific hypothesis on its shape and without separating the perturbative and non-perturbative components.

  The charm and anti-charm PDFs are considered to be equal, since there is currently no data which can constrain their difference.

  Even if there are significant errors, in the large x region one can find a little bump which is supposed to be the intrinsic component of the charm.

  Again, the mean value is obtained from the central PDF while the error is given by the standard deviation.

It is now possible to analyse the plots 5.9 and 5.10. The $\mathcal{O}(\alpha_s^3)$ matching defines a PDF with a peak that is significantly higher than the second order matching PDF: this is clearly due to the important increase in the gluon contribution we previously described both in N-space and x-space. Even if the missing terms make the peak lower down, we do not expect them to reduce it at almost one third of its actual value.

The two plots show that the α_s^3 matching and the α_s^2 matching have a very similar shape: we thus found an important NLO correction with the same shape of the leading order. This means that the perturbative series is still far from convergence and the error of the perturbative charm is thus totally unreliable. What is really needed at the moment is waiting for the calculation of the missing terms in A_{Qg}, in order to obtain a correct numerical result and verify if there are important cancellations that modify significantly our result. We expect that even including these terms, the new result will not be so different from ours, so at this point a 4-loop matching would be crucial. Actually such a calculation is totally inaccessible: an important conceptual breakthrough would be needed.

As things stand, it is clear that a 2-loop matching charm is no longer reliable. Basically, one can consider two different options: firstly, one can consider the charm PDF as the one obtained with a α_s^3 matching f_c^3 with an error bar given by the difference between the α_s^2 and the α_s^3 PDFs, that is $\delta f_c = f_c^3 - f_c^2$. In this way, the new charm PDF partially covers the upper error bar of the fitted charm, which leads to suppose that the *true* charm can be in this region. The second option is in fact fitting the charm PDF, with the awareness that probably the real charm can be better described by the upper error bar than by the fitted central value.

Chapter 6

Conclusions

This thesis provides a detailed description of the so-called Fixed-Order Next-Leading-Log FONLL approach which defines a general framework for the inclusion of heavy quark mass contributions to deep-inelastic structure functions. We developed the FONLL equations up to α_s^3, which means one order higher than the actually used ones, with the basic idea of completely defining - at least theoretically - the FONLL framework at the new frontier for high-precision predictions. We then studied in detail the matching condition of the heavy quark, considering the explicit case of the charm PDF, providing a first phenomenological result at α_s^3.

In the first part of this work, we briefly revised basic concepts of QCD in the case of massless quarks, in order to explain why the treatment of heavy quarks is not trivial.

The second chapter is dedicated to a discussion on how to treat heavy quarks using a Fixed Flavour Number Scheme or a Variable Flavour Number Scheme, highlighting the different accuracy on the whole kinematic region and the perturbative matching relations between the two schemes. We also introduced the concepts of perturbative and heavy quark component, which naturally leads to focus on the charm quark, whose mass is close to the scale where one would expect a non perturbative behaviour to manifest.

At this point, the FONLL approach is presented. Firstly, we described the FONLL methodology for the construction of DIS structure functions: basically, FONLL structure functions can be constructed expanding out the massless equations and then substituting a finite number of terms with their massive counterparts. Any double counting is then subtracted: they are con-

stant and logarithmic terms that are both resummed in the massless scheme and explicitly present in the massive one. The final result now presents a fixed order accuracy, thanks to the number of orders that that have been included in perturbation theory, and a logarithmic accuracy, due to the resummation of large logarithms in the massless scheme. FONLL equations correctly reproduce the massless scheme results in the high energy region $Q^2 \gg m_h^2$ and the massive one at threshold $Q^2 \sim m_h^2$.

The FONLL structure functions are explicitly calculated in the case of a DIS electromagnetic interaction at α_s^3. In order to obtain the structure functions, we explicitly studied the matching relations between the massless and the massive schemes for the running coupling and the PDFs. We then calculated the structure functions without providing any numerical result because many massive Wilson coefficients that are required are analytically known in the asymptotic region only. Actually, a great effort is dedicated to the calculation of these terms [11, 12] and, probably, a full α_s^3 matching will be performed in the next few years.

We then provided a detailed analysis of the heavy quark PDF. In this thesis, we worked under the assumption of a fully perturbative heavy quark, which can be unsatisfactory when considering the charm. The charm, in fact, has a mass similar to the proton's, which leads to suppose the existence of a non negligible intrinsic component. The actual knowledge of the charm PDF is described by figure 4.3: the fully perturbative charm, which is known exactly up to α_s^2, results particularly different than the fitted charm. Adding the α_s^3 correction means considering the first non trivial contribution the the leading order.

The computation required the calculation of two OMEs, A_{Qq} and A_{Qg}, which has been obtained in N-space directly from the authors. After a preliminary analysis in both N- and x-space, we obtained the charm PDF at α_s^3: we found a significant increase in the PDF, due to the gluon contribution. In particular, we obtained an important NLO correction with the same shape of the leading order, which means that the perturbative series is far from convergence. It must be remarked that our result is only partial because the required OMEs are not fully known; anyway, the most significant part has already been computed, which is sufficient for a first phenomenological study.

Our result clearly shows that the α_s^2 charm PDF is unreliable. For studying the charm content of the proton one can thus consider two different options: the first one is considering the charm PDF as the 3-loop matching PDF, with an error bar that covers the difference between the α_s^2 PDF and

the α_s^3 one. The second option is fitting the charm: with the awareness of the 3-loop matching result, one can suppose that the real charm PDF can be better described by a PDF in the upper error bar than by the fitted central value.

In order to complete the work presented in this thesis, a full matching at α_s^3 with the complete A_{Qg} term should be performed. This way, one would verify exactly how the missing terms modify our result. As already stated, we believe that these missing terms will not modify substantially the charm PDF, leading to the necessity for a 4-loop matching contribution. The calculation of the α_s^4 correction is totally inaccessible at the moment and it will probably require many years for its completion. At the moment, the best options we have are for studying the charm PDF is considering the fitted charm or the 3-loop perturbative charm with an important error bar as described before.

Bibliography

[1] S.Forte, E.Laenen, P.Nason, J.Rojo, Nucl. Phys. B 834 (2010), 116.

[2] S.A.Larin, T. van Ritbergen, J.A.M. Vermaseren, Nucl. Phys. B 438 (1995), 278.

[3] M.Hoschele, J.Hoff, A.Pak, M.Steinhauser, T.ueda, Phys. Lett. B 721 (2013), 244.

[4] M.Buza, Y.Matiounine, J.Smith, W.L. van Neerven, Eur. Phys. J. C 1 (1998) 301.

[5] J.Ablinger, A.Behring, J.Blümlein, A.De Freitas, A.Hasselhuhn, A. von Manteuffel, M.Round, C.Schneider, F.Wißbrock, DESY 13–210, hep-ph/1406.4654.

[6] J.Ablinger, J.Blümlein, A. De Freitas, A.Hasselhuhn, A. von Manteuffel, M.Round, C.Schneider, F.Wissbrock, DESY 13–185, hep-ph/1402.0359.

[7] J.Blümlein, A.Hasselhuhn, S.Klein, C.Schneider, DESY 12-055, hep-ph/1205.4184.

[8] J. Ablinger, J. Blümlein, A. De Freitas, A. Hasselhuhn, A. von Manteuffel, M. Round, C. Schneider, DESY 14-018, hep-oh/1405.4259.

[9] M.Höschele, J.Hoff, A.Pak, M.Steinhauser, T.Ueda, hep-ph/1211.6559v1.

[10] S.Buehler, A.Lazopoulos, hep-ph/1306.2223.

[11] J.Ablinger, A.Behring, J.Blümlein, A. De Freitas, A. von Manteuffel, C.Schneider, hep-ph/1409.1135

[12] A. Behring, I. Bierenbaum, J. Blumlein, A. De Freitas, S. Klein, and F. Wißbrock, hep-ph/1403.6356

[13] J. Ablinger, A. Behring, J. Blümlein, A. De Freitas, A. von Manteuffel, C. Schneider, hep-ph/1711.07957v1

[14] W.Tung, H.Lai, A.Belayev, J.Pumplin, D.Stump, et al., JHEP vol. 0702 (2007), p.053

[15] J.C.Collins, Phys. Rev. D 58 (1998), 09002.

[16] M.Kramer, F.I.Olness, D.E.Soper, Phys. Rev D 62 (2000), 096007

[17] A.Martin, W.Stirling, R.Thorne, G.Watt, Phys. Lett. B 652 (2007), 292.

[18] R.Thorne, R.Roberts, Phys. Rev. D 57 (1998), 6871.

[19] M.Cacciari, M.Greco, P.Nason, JHEP 9805 (1998), 007.

[20] C.Duhr, F.Dulat, V.Hirschi, B.Mistlberger, hep-ph/2004.04752 (2020).

[21] S.J.Brodsky, P.Hoyer, C.Peterson, N.Sakai, Phys. Lett. B 93 (1980), 451.

[22] S.J.Brodsky, C.Peterson, N.Sakai, Phys. Rev. D 23 (1981), 2745.

[23] T.Stavreva, I.Schienbein, F.Arleo, K.Kovarik, F.Olness, J.Y.Yu, J.F.Owens, JHEP 01 (2011), 152.

[24] V.A.Bednyakov, M.A.Demichev, G.I.Lykasov, T.Stavreva, M.Stockton, Phys. Lett. B 728 (2014), 602.

[25] R.D.Ball, V.Bertone, M.Bonvini, S.Forte, P.G.Merrild, J.Ruojo, L.Rottoli, Phys. Lett. B 754 (2016), 49.

[26] R.K.Ellis, W.J.Stirling, B.R.Webber, *QCD and Colider Physics*, Cambridge University Press.

[27] K.G.Chetyrkin, F.V. Tkachov, Nucl. Phys. B 192 (1981), 159.

[28] A.Buckley, J.Ferrando, S.Lloyd, K.Nordström, B.Page, M.Rüfenacht, M.Schönherr, G.Watt, The European Physical Journal C 75 (2015), 132.

[29] NNPDF collaboration, hep-ph/1706.00428.

[30] W.N.Bailey, Generalized Hypergeometric Series, (Cambridge University Press, Cambridge, 1935).

[31] E.W.Barnes, Proc. Lond. Math. Soc. (2) 6 (1908), 141.

[32] A.V.Kotikov, Phys. Lett. B 254 (1991), 158.

[33] J.Ablinger, *A Computer Algebra Toolbox for Harmonic Sums Related to Particle Physics*, Johannes Kepler University (2009).

[34] E.Remiddi, J.A.M.Vermaseren, Int. J. Mod. Phys. A 15 (2000), 725.

[35] J. Vollinga, Nucl.Instrum.Meth. A559 (2006), 282-284.

[36] N.Karjanto, math.HO/2002.01342 (2020).

[37] M.A.G.Aivazis, F.I.Olness,W.Tung Phys. Rev. D 50 (1994), 3085.

[38] C.Anastasiou, C.Duhr, F.Dulat, F.Herzog, B.Mistlberger, Rev. Lett. 114 (2015), 212001.

[39] F.A.Dreyer,A.Karlberg, Phys.Rev. Lett.117 (2016),072001

[40] J.A.M.Vermaseren, A.Vogt, and S.Moch, Nucl. Phys.B 724 (2005), 3.

[41] T.Kinoshita, J. Math. Phys. 3 (1962), 650.

[42] T.D.Lee, M.Nauenberg, Phys. Rev. 133 (1964), B1549.

[43] G.Altarelli, G.Parisi, Nucl. Phys. B 126 (1977), 298.

[44] F.Herzog, B.Ruijl, T.Ueda, J.A.M.Vermaseren, A.Vogt, Journal of High Energy Physics 2017, 90 (2017).

[45] Particle Data Group, Review: Quantum Chromodynamics (2020).

[46] J.Ablinger, J. Blümlein, math-ph/1304.7071

[47] J. Blümlein, Computer Physics Communications 180, 11 (2009).

[48] GSL-GNU scientific library, www.gnu.org/software/gsl/

[49] M.E.Peskin, D.V.Schroeder, *An introduction to Quantum Field Theory*, Westview Press (1995)

[50] P.Nogueira, J. Comput. Phys. 105 (1993) 279.

[51] S.Laporta, Int. J Mod. Phys. A 15 (2000) 5087.

Acknowledgements

Vorrei ringraziare tutti coloro che hanno contribuito alla stesura di questo elaborato e che mi hanno supportata in questi meravigliosi anni universitari.

Ringrazio il Professor Stefano Forte, per l'immensa passione che mi ha trasmesso. Non posso che ringraziarlo infinitamente per la disponibilità dimostratami in questo progetto di tesi. Lavorare con lui è stato un piacere.

Ringrazio il Professor Stefano Carrazza, perchè ha saputo guidarmi con pazienza nel mondo della computazione.

Un immenso grazie ai miei compagni di viaggio Carlo, Davide, Giorgia e Alessandro: condividere con voi questi cinque anni è stato bellissimo. Siete stati i compagni migliori che potessi chiedere. A breve saremo sparpagliati per il mondo ma sono certa che tra di noi non cambierà nulla. Vi aspetto a Monaco!

Un ringraziamento importante lo devo anche a quelle amiche che, pur non vedendole spesso, sono sempre con me: Chiara e Anita, grazie mille per tutto.

Grazie anche a Beatrice, Melania, Elena, Marco e Rox: la disponibilità che mi avete dimostrato è impagabile.

Un grazie speciale va ai miei genitori, perchè mi hanno sempre lasciata libera di compiere le mie scelte, accompagnandomi in ogni mia decisione. Grazie anche a mio fratello Simone, per il suo tacito supporto.

Grazie ai miei nonni, perchè anche se non hanno ben capito che cosa io stia facendo, sono sempre orgogliosi dei miei risultati.

Per ultimo, ma sicuramente non per importanza, un grazie enorme a Daniele: senza di lui sarebbe tutto diverso.